

A Statistical Recurrent Stochastic Volatility Model for Stock Markets

T.-N. Nguyen, M.-N. Tran, D. Gunawan, R. Kohn*

January 25, 2022

Abstract

The Stochastic Volatility (SV) model and its variants are widely used in the financial sector while recurrent neural network (RNN) models are successfully used in many large-scale industrial applications of Deep Learning. Our article combines these two methods in a non-trivial way and proposes a model, which we call the Statistical Recurrent Stochastic Volatility (SR-SV) model, to capture the dynamics of stochastic volatility. The proposed model is able to capture complex volatility effects (e.g., non-linearity and long-memory auto-dependence) overlooked by the conventional SV models, is statistically interpretable and has an impressive out-of-sample forecast performance. These properties are carefully discussed and illustrated through extensive simulation studies and applications to five international stock index datasets: The German stock index DAX30, the Hong Kong stock index HSI50, the France market index CAC40, the US stock market index SP500 and the Canada market index TSX250. An user-friendly software package together with the examples reported in the paper are available at <https://github.com/vbayeslab>.

Keywords. Deep Learning; volatility modelling, recurrent neural networks, financial econometrics.

1 Introduction

The volatility of a financial time series, such as stock returns, is defined as the variance of the returns and serves as a measure of the uncertainty about the returns. The volatility, which is of great interest to financial econometricians, is unobserved and therefore often modelled statistically in order to estimate it. The two model classes most frequently used in volatility modelling are the Generalized Autoregressive Conditional Heteroscedastic (GARCH) models and the Stochastic Volatility (SV) models. The GARCH model (Bollerslev, 1986) expresses the current volatility, conditional on the previous returns and volatilities, as a *deterministic* and linear function of the squared returns and the conditional volatilities in the previous time period. The SV model (Taylor, 1982, 1986), on the other hand, uses a latent stochastic

***Nguyen** and **Tran**: Discipline of Business Analytics, University of Sydney Business School and ACEMS. **Gunawan**: School of Mathematics and Applied Statistics, University of Wollongong and ACEMS. **Kohn**: School of Economics, UNSW Business School and ACEMS.

process to model the volatility, which is usually taken as a first order autoregressive process. It is well documented that the GARCH and SV models are able to capture important effects exhibited in the variance of financial returns. For example, the volatilities in financial returns are observed to be highly autocorrelated in certain time periods and exhibit periods of both low and high volatility (Mandelbrot, 1967). This so-called volatility clustering phenomenon can be modeled by the volatility processes introduced in the GARCH and SV models, making these volatility models widely employed in financial time series modelling.

Although the GARCH and SV models were independently and almost concurrently introduced, the GARCH models were initially more widely adopted as it is much easier to estimate GARCH models than SV models. This is because the likelihood of a GARCH model can be obtained explicitly, while the likelihood of a SV model is intractable as it is an integral over the latent process. However, the conditional variance process of GARCH models is deterministic and hence GARCH models might not capture efficiently the random oscillatory behavior of financial volatility (Nelson, 1991). SV models are considered as an attractive alternative to GARCH models because they overcome this limitation (Kim et al., 1998; Yu, 2002). Recent advances in Bayesian computation such as particle Markov chain Monte Carlo (PMCMC) (Andrieu et al., 2010) allow straightforward estimation and inference for SV models.

Standard SV models still cannot appropriately capture some important features arising in financial volatility. For example, a large amount of both theoretical and empirical evidence indicates that there exists long-range persistence in the volatility process of many financial returns, see, e.g, Lo (1991), Ding et al. (1993), Crato and de Lima (1994) and Bollerslev and Mikkelsen (1996). The long-memory property of a time series implies that the decay of the autocorrelations of the series is slower than exponential. The standard SV model of (Taylor, 1982) uses an AR(1) process to model the log of the volatility and hence might fail to capture this type of persistence (Breidt et al., 1998). Another line of the literature shows strong evidence of non-linear auto-dependence in the volatility process of some stock and currency exchange returns (Kiliç, 2011) and that the simple linear AR(1) process cannot effectively capture the underlying non-linear volatility dynamics.

Breidt et al. (1998) proposed the Long Memory Stochastic Volatility (LMSV) model to overcome the short-memory limitation of the standard SV model. LMSV uses an ARFIMA process (Granger and Joyeux, 1980) as an alternative to the AR(1) process to capture the long-memory dependence in the volatility. The empirical evidence in Breidt et al. (1998) suggests that the LMSV model is able to capture the long-memory volatility behaviour in some stock return datasets. However, the literature is unclear about whether the LMSV model can capture non-linear dynamics within the volatility process, because the ARFIMA model is linear. Additionally, it is challenging to estimate the LMSV model as its likelihood is intractable. We are unaware of any available software package that implements the LMSV methodology. In another approach, Yu et al. (2006) introduced a family of non-linear SV (N-SV) models to capture the possible departure from the log transform commonly used in SV models. In the standard SV model, the logarithm of volatility is assumed to follow an AR(1) process; N-SV uses other non-linear transformations, such as the Box-Cox power function, rather than the logarithm. The simulation studies and empirical results on currency exchange and option pricing data in Yu et al. (2006) show that the N-SV model using the Box-Cox transformation is able to detect some interesting effects in the underlying volatility process. The general use of N-SV models requires the user to select an appropriate non-linear

transformation for the dataset under consideration, and this might lead to a challenging model selection problem. Neither Breidt et al. (1998) nor Yu et al. (2006) clearly discussed the out-of-sample forecast performance of their LMSV and N-SV models.

Recurrent neural networks (RNN) in the Deep Learning literature have impressive prediction performance and have been successfully deployed in a large number of industrial-level applications (language translation, image captioning, speech synthesis, etc.). The RNN models are well-known for their ability to efficiently capture the long-range memory and non-linear dependence existing within various types of sequential data, and are considered as the state-of-the-art models for many sequence learning problems (Lipton et al., 2015). Many researchers and practitioners have used RNN for mean modelling in financial time series analysis, but the general consensus is that these machine learning models do not clearly outperform the traditional time series models such as ARMA and ARIMA (see, e.g., Makridakis et al. (2018) and Zhang (2003)). Makridakis et al. (2018) note that without careful modifications, Machine Learning models are usually less accurate than the statistical approaches that have been extensively investigated in the financial time series literature. Recently, the idea of using the RNN models to improve the predictive performance of GARCH-type models has also been proposed for volatility modelling. For example, Kim and Won (2018) use the volatility estimates from several GARCH-type models as inputs to a RNN model, which then non-linearly transforms these inputs to output the final estimate of the volatility. The empirical results on the Korean stock market KOSPI 200 index show a significant improvement of forecast performance of the proposed hybrid model over several GARCH-type benchmark models. However, similar to many engineering-oriented Machine Learning models, Kim and Won’s model overlooks the interpretation aspect in volatility modelling, which is often of main interest to econometricians. One of the main motivations of our article is to develop deep learning based volatility models that are not only able to produce accurate prediction, but also interpretable and have meaningful in-sample analysis. These models should not overlook the well-established features of traditional econometric models, that are motivated by the well-known stylized facts in financial time series such as volatility clustering and fat tails.

In the SV literature, there is still lack of research using RNN structures to model the stochastic volatility dynamics of financial time series, perhaps because of two reasons. First, it is non-trivial to sensibly incorporate RNN into the statistical volatility models. Simple adaptations of RNN to volatility models easily overlook the important stylized facts exhibited in financial volatility, which are well captured by the AR(1) process in the SV model. It is important to select appropriate RNN structures that are not only able to produce accurate out-of-sample volatility forecast, but also explain well the volatility dynamics. Second, a stochastic volatility model that incorporates a RNN structure into its latent stochastic process is highly sophisticated and thus challenging to estimate.

This paper combines the SV and RNN models in a non-trivial way, and proposes a new model, called the Statistical Recurrent Stochastic Volatility (SR-SV) model. In particular, we use the Statistical Recurrent Unit (SRU) structure of Oliva et al. (2017), which is a special type of RNN models, to capture complex volatility effects overlooked by an AR(1) process in the standard SV model but still retain the essential components of the SV model. This combination allows the SR-SV model to enjoy much of advances from both worlds of deep learning (e.g., flexibility and excellent predictive performance) and econometric volatility modelling (e.g., excellent interpretability of volatility effects). The SR-SV model belongs to

the class of parametric state space models whose Bayesian inference can be performed using recent advances in the Sequential Monte Carlo (SMC) and particle MCMC literature (Andrieu and Roberts, 2009; Andrieu et al., 2010; Duan and Fulop, 2015; Deligiannidis et al., 2018). The simulation studies and empirical results on the five stock index datasets demonstrate that the SR-SV model can efficiently capture the potential non-linear and long-memory effects in the underlying volatility dynamics, and provide better out-of-sample forecasts than the standard SV, N-SV and LMSV models. We note that we have tested SR-SV on a wider range of stock returns but only report in the paper the results for five of them, as we constantly observed a similar improvement of the model compared to the other three counterpart. A Matlab software package implementing Bayesian estimation and inference for SR-SV together with the examples reported in this paper are available on github¹.

The article is organized as follows. Section 2 briefly reviews the SV and SRU models, and presents the SR-SV model. Section 3 discusses in detail Bayesian estimation and inference for the SR-SV model. Section 4 presents the simulation study and applies the SR-SV model to analyze the five stock index datasets. Section 5 concludes. The Appendix gives details of the implementation and further empirical results.

2 The SR-SV model

2.1 The SV model and its possible weaknesses

Let $y = \{y_t, t = 1, \dots, T\}$ be a series of financial returns. We consider a basic version of SV models (Taylor, 1982)

$$z_t = \mu + \phi(z_{t-1} - \mu) + \epsilon_t^z, \quad \epsilon_t^z \sim \mathcal{N}(0, \sigma^2), \quad t = 2, \dots, T, \quad z_1 \sim \mathcal{N}\left(\mu, \frac{\sigma^2}{1 - \phi^2}\right), \quad (1)$$

$$y_t = e^{\frac{1}{2}z_t} \epsilon_t^y, \quad \epsilon_t^y \sim \mathcal{N}(0, 1), \quad t = 1, 2, \dots, T. \quad (2)$$

The persistence parameter ϕ is assumed to be in $(-1, 1)$ to enforce stationarity of both the z and y processes. In this SV model, the log volatility process z is assumed to follow an AR(1) model. It is well documented in the financial econometrics literature that financial time series data often exhibit a long-term auto-dependence, which forces the persistence parameter ϕ to be close to 1 (Jacquier et al., 1994; Kim et al., 1998). Write $p(z|\theta)$ for the density of z given the model parameters $\theta = (\mu, \phi, \sigma^2)$ and $p(y|z)$ for the density of the data y conditional on z . We can view $p(z|\theta)$ as the prior with θ being the hyper-parameters and $p(y|z)$ as the likelihood (Jacquier et al., 1994). Under this perspective, the SV model (1)-(2) puts non-zero prior mass on AR(1) stochastic processes, and zero or almost-zero mass on stochastic processes that are far from being well approximated by an AR(1). This means that the SV model in (1)-(2) might not be able to capture more complex dynamics in the posterior behavior of the log volatility process z , such as long-term memory or non-linear auto-dependence, and that a more flexible prior distribution should be put on z . We will design such a flexible prior by combining the attractive features from both SV and RNN time series modeling techniques.

Yu et al. (2006) propose a class of non-linearity N-SV models as a variant of SV which allows a more flexible link between the variance $\text{Var}(y_t|z_t)$ and the AR(1) process z . Their

¹The link is provided in the unblinded version.

N-SV model, using the Box-Cox transformation for $\text{Var}(y_t|z_t)$, is written as

$$z_t = \mu + \phi(z_{t-1} - \mu) + \epsilon_t^z, \quad \epsilon_t^z \sim \mathcal{N}(0, \sigma^2), \quad t = 2, \dots, T, \quad z_1 \sim \mathcal{N}\left(\mu, \frac{\sigma^2}{1 - \phi^2}\right), \quad (3)$$

$$y_t = (1 + \delta z_t)^{1/2\delta} \epsilon_t^y, \quad \epsilon_t^y \sim \mathcal{N}(0, 1), \quad t = 1, 2, \dots, T, \quad (4)$$

where δ is the auxiliary parameter that measures the degree of non-linearity rather than the log transform. As $\delta \rightarrow 0$, $(1 + \delta z_t)^{1/2\delta} \rightarrow e^{\frac{1}{2}z_t}$ and hence the N-SV model includes the SV model as a special case. The term non-linearity here might cause some confusion, as it does not refer to the non-linear auto-dependence within the log volatility process z , but the non-linearity between $\text{Var}(y_t|z_t)$ and z_t .

Breidt et al. (1998) suggest to use an ARFIMA(p, d, q) process (Granger and Joyeux, 1980; Hosking, 1981) for the log volatility z_t to capture the long-memory auto-dependence exhibited in financial time series. Their LMSV model is written as

$$(1 - B)^d \Phi(B) z_t = \Theta(B) \eta_t, \quad \eta_t \sim \mathcal{N}(0, \sigma_\eta^2), \quad (5)$$

$$y_t = \sigma_t \epsilon_t, \quad \sigma_t = \kappa e^{\frac{1}{2}z_t}, \quad \epsilon_t \sim \mathcal{N}(0, 1), \quad t = 1, 2, \dots, T, \quad (6)$$

where $\Phi(B) = 1 - \phi_1 B - \phi_2 B^2 - \dots - \phi_p B^p$, $\Theta(B) = 1 + \theta_1 B + \theta_2 B^2 + \dots + \theta_q B^q$, and B is a backshift operator, i.e., $B^s X_t = X_{t-s}$. To ensure the stationarity and invertability of the log volatility process z_t , the fractional integration parameter d is assumed to be in $(-0.5, 0.5)$ and the roots of $\Phi(B)$ and $\Theta(B)$ have to lie outside the unit circle.

Another notable line of research in the SV literature is the class of semi-parametric stochastic volatility models that incorporate non-parametric techniques into modelling the conditional distribution of financial returns. For example, the stochastic volatility, Dirichlet process mixture (SV-DPM) model of Jensen and Maheu (2010) uses a Dirichlet process prior (Ferguson, 1973) to characterize the conditional distribution of y_t . Semi-parametric models are different from the SR-SV model in two important aspects. First, the SV-DPM model is proposed to capture the asymmetries and leptokurtotic behaviors of financial returns, while the SR-SV model focuses on modeling the non-linearity and long-memory auto-dependence in the log-volatility dynamics. Second, the SV-DPM model is a semi-parametric model in the sense that the model cannot be described using a finite number of parameters as it uses a non-parametric prior, e.g. Dirichlet process, to simulate the conditional return and retains the parametric structure, e.g. AR(1), of the log-volatility in the standard SV model. The SR-SV model, on the other hand, is a parametric model with eleven parameters whose mathematical representation will be discussed in Section 2.3. Our article therefore uses parametric models including the standard SV, N-SV and LMSV models as the benchmarks to evaluate the SR-SV model.

2.2 The SRU model

There are at least two approaches to modeling time series data. One approach is to represent time effects *explicitly* via some simple function, often a linear function, of the lagged values of the time series. This is the mainstream time series data analysis approach in the statistics literature with the well-known models such as AR or ARMA. The alternative approach is to represent time effects *implicitly* via latent variables, which are designed to store the memory of the dynamics in the data. These latent variables, also called hidden states, are updated

in a recurrent and deterministic manner using the information carried over by their values from the previous time steps and the information from the data at the current time step. Recurrent neural networks (RNN), belong to the second category, were first developed in cognitive science and successfully used in computer science and other fields. Another class of models that represent time implicitly is state space models, albeit the recurrent update is stochastic, which are widely used in econometrics and statistics. The SV model discussed in Section 2.1 is an example of state space models.

For the purpose of this section, we denote the time series data as $\{D_t = (x_t, z_t), t = 1, 2, \dots\}$ where x_t is the vector of inputs and z_t the scalar output. In our article, it is useful to think of x_t as scalar; however, the RNN approach is often efficiently used to model multivariate time series. If the time series of interest has the form $\{z_t, t = 1, 2, \dots\}$, it can be written as $\{(x_t, z_t), t = 1, 2, \dots\}$ with $x_t = z_{t-1}$. Our goal is to model the conditional distribution $p(z_t | x_t, D_{1:t-1})$. If the serial dependence structure is ignored, then a feedforward neural network (FNN) can be used to transform the raw input data x_t into a set of hidden units h_t , also called *learned features* or *summary statistics*, for the purpose of explaining or predicting z_t . However, this approach is unsuitable for time series data as the time effects or the serial dependence are totally ignored. The main idea behind RNN is to let the set of hidden units h_t to feed itself using its lagged value h_{t-1} from the previous time step $t-1$. Hence, RNN can be best thought of as a FNN that allows a connection of the hidden units to their value from the previous time step, enabling the network to possess memory. Mathematically, this RNN model (Elman, 1990) is written as

$$h_t = \Psi(w_x x_t + w_h h_{t-1} + b), \quad (7)$$

$$\eta_t = \beta_0 + \beta_1 h_t, \quad (8)$$

$$z_t | \eta_t \sim p(z_t | \eta_t). \quad (9)$$

The model parameters include w_x, w_h, b, β_0 and β_1 , $\Psi(\cdot)$ is a non-linear activation function, e.g., common choices are the *sigmoid* $\Psi(z) = 1/(1 + e^{-z})$ and the *tanh* $\Psi(z) = (e^z - e^{-z})/(e^z + e^{-z})$, and $p(z_t | \eta_t)$ is a probability density depending on the learning task. For example, if z_t is continuous, then typically $p(z_t | \eta_t)$ is a Gaussian density with mean η_t ; if z_t is binary, then $z_t | \eta_t$ follows a Bernoulli distribution with probability $\Psi(\eta_t) = 1/(1 + e^{-\eta_t})$. Usually one sets $h_1 = 0$, i.e. the neural network initially does not have any memory.

Figure 1 illustrates graphically the RNN model (7)-(9). We follow Goodfellow et al. (2016) and use a black square to indicate the delay of a single time step in the circuit diagram (*left*). The circuit diagram can be interpreted as an unfolded computational graph (*right*), where each node is associated with a particular time step.

The unfolded graph in Figure 1 suggests that the hidden state at time t is the output of a composite function

$$h_t = f\left(x_t, f(x_{t-1}, \dots, f(x_1, h_0))\right), \text{ where } f(x_t, h_{t-1}) := \Psi(w_x x_t + w_h h_{t-1} + b), \quad (10)$$

which somewhat resembles a multiplication structure in terms of the weight w_h . Consequently, the gradient of h_t with respect to the model parameters might either explode or vanish if t is sufficiently large and w_h is not equal to 1, and hence making it inefficient for the Simple RNN model to learn in long time series. See Goodfellow et al. (2016) for further explanation.

Many sophisticated RNN structures have been proposed to overcome the aforementioned problem in the Simple RNN model; for example, the Long Short-term Memory model of

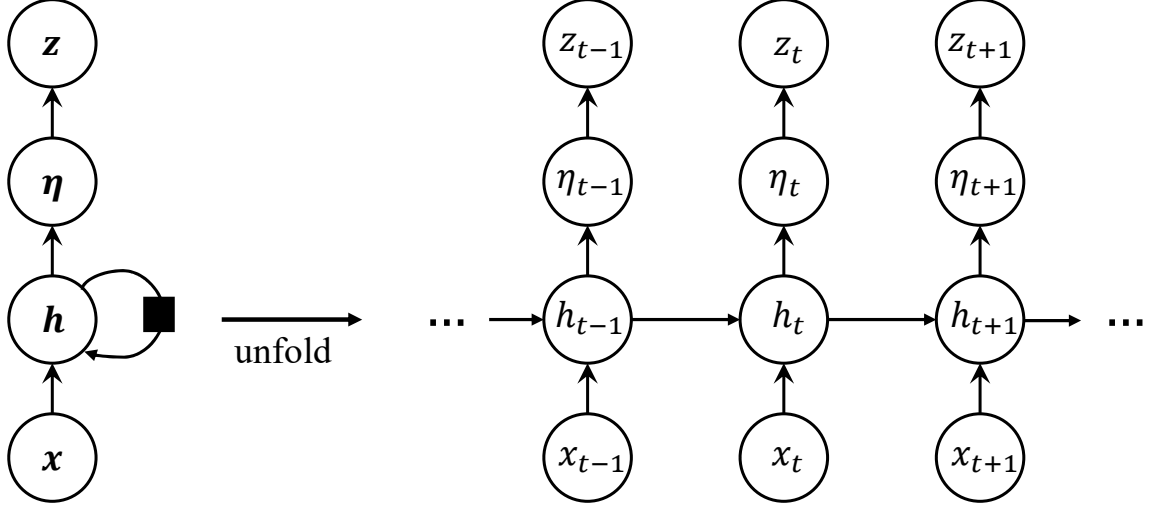


Figure 1: Graphical representation of the RNN model in (7)-(9).

Hochreiter and Schmidhuber (1997), the Gated Recurrent Unit of Cho et al. (2014) and the Statistical Recurrent Unit (SRU) of Oliva et al. (2017). The SRU allows the vector of summary statistics h_t to traverse through the network using a moving average. We will use the SRU in this paper as its structure and some of its main parameters carry statistical meaning; see Section 2.3. A general SRU structure is mathematically written as

$$r_t = \Psi(W_h h_{t-1} + b_r), \quad (11a)$$

$$\varphi_t = \Psi(W_r r_t + W_x x_t + b_\varphi), \quad (11b)$$

$$h_t^{(\alpha_j)} = \alpha_j h_{t-1}^{(\alpha_j)} + (1 - \alpha_j) \varphi_t, j = 1, \dots, m; h_t = (h_t^{(\alpha_1)}, \dots, h_t^{(\alpha_m)})^\top, \quad (11c)$$

where $\alpha = (\alpha_1, \dots, \alpha_m) \in (0, 1)$ is a vector of moving average weights, and W_h , b_r , W_r , W_x and b_φ are the model parameters. We denote the functional learning structure in (11a)-(11c) as $h_t = \text{SRU}(x_t, h_{t-1})$, which takes x_t - the input data at current time t - and h_{t-1} - the previous output of the SRU - as the input arguments. See Figure 2(a) for the graphical representation of this SRU structure. The moving average structure of the state h_t allows the RNN network with SRU units to enjoy some advantages compared to other RNN models. The current state h_t is related to the previous state h_{t-1} both *directly* and *indirectly* and hence mitigate the problem of multiplying the same quantities multiple times as in the Simple RNN model. The novel architecture of the SRU allows the model to capture long term dependencies in data via simple moving averages.

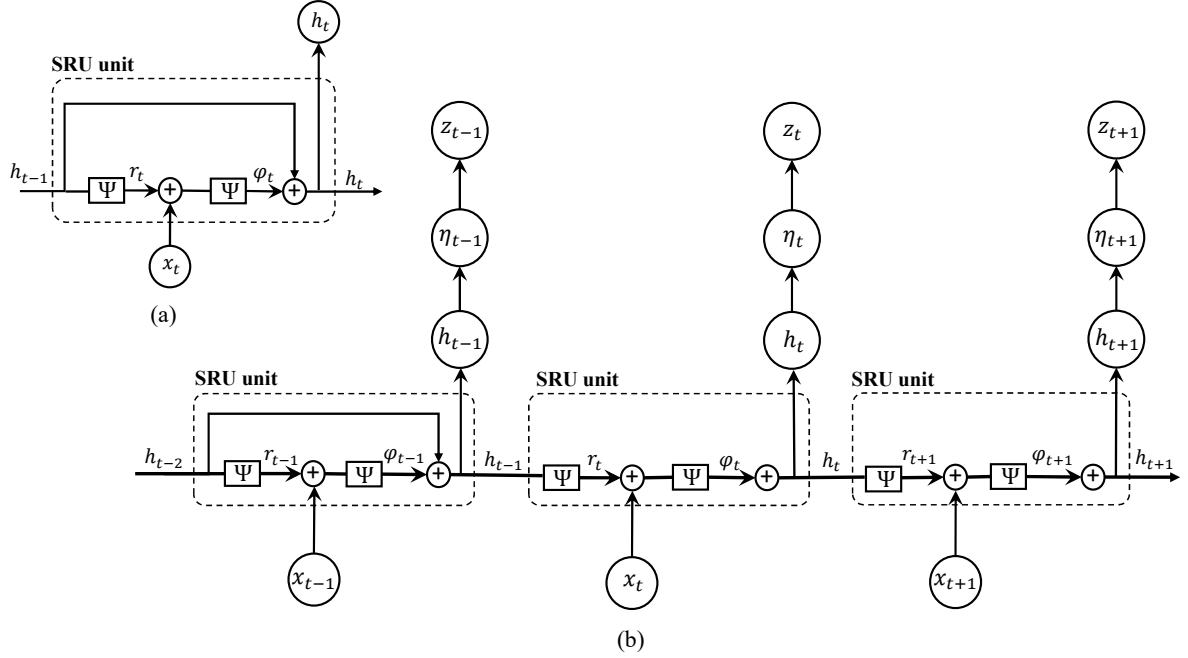


Figure 2: The structure of the SRU unit (a) and the graphical representation of the SRU model (b), which uses the SRU unit to compute the latent state h_t .

2.3 The SR-SV model

This section proposes the SR-SV model that combines SV and SRU for financial volatility modelling. The key idea is that we use the SRU structure to capture the complicated effects such as long-term memory and non-linear auto-dependence, in the volatility dynamics that are overlooked by the basic SV models. This leads to a prior distribution for the log volatility process z that is much more flexible than the AR(1) prior (c.f. Section 2.1). Our proposed SR-SV model is as follows

$$h_t = \text{SRU}(x_t, h_{t-1}), \quad t = 2, \dots, T, \quad \text{with } h_1 := 0, \quad x_t = (\eta_{t-1}, z_{t-1})^\top, \quad (12)$$

$$\eta_t = \beta_0 + \beta_1 h_t + \epsilon_t^\eta, \quad \epsilon_t^\eta \stackrel{iid}{\sim} \mathcal{N}(0, \sigma^2), \quad t = 1, \dots, T, \quad (13)$$

$$z_t = \eta_t + \phi z_{t-1}, \quad t = 1, \dots, T, \quad (14)$$

$$y_t = e^{\frac{1}{2} z_t} \epsilon_t^y, \quad \epsilon_t^y \stackrel{iid}{\sim} \mathcal{N}(0, 1), \quad t = 1, 2, \dots, T, \quad (15)$$

that is, we use a SRU to model the dynamics of the hidden states h_t . Here, z_0 is the initial value of the log volatility process and a convenient choice of z_0 is the log of the unconditional variance of the observed series y , i.e., $z_0 = \log(\text{var}(y))$. We follow the literature to initialize $h_1 = 0$ as the recurrent units initially have no memory. Figure 3 plots the graphical representation of the SR-SV model. See Appendix A.2 for the fully-written version of the SR-SV model.

We note the following important properties of the SR-SV model. First, the SR-SV model in (12)-(15) retains the measurement equation (15) and the linear part ϕz_{t-1} of the AR(1) process from the standard SV model, and captures the volatility effects not captured by the AR(1) process, e.g. non-linear and long-memory auto-dependence, via the latent state h_t of

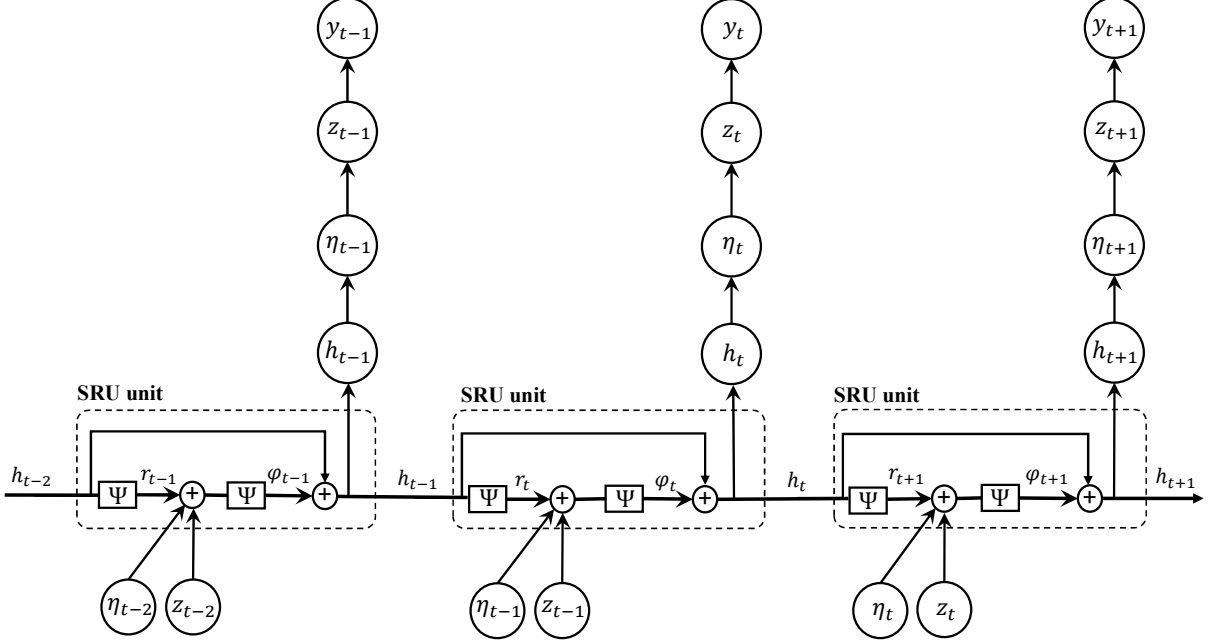


Figure 3: Graphical representation of the SR-SV model. The \oplus symbol represents the addition operation.

the SRU structure. The log volatility at time t in (14) can be written as

$$z_t = \beta_0 + \beta_1 \text{SRU}(\eta_{t-1}, z_{t-1}, h_{t-1}) + \phi z_{t-1} + \epsilon_t^\eta. \quad (16)$$

Therefore, the parameter β_1 characterizes all the effects in the underlying log volatility process z rather than the short-term linear effect captured by the AR(1) process. We refer to β_1 as the *non-linearity long-memory* coefficient. If $\beta_1 = 0$ and $\epsilon_1^\eta \sim \mathcal{N}(\beta_0/(1-\phi), \sigma^2/(1-\phi^2))$, the SR-SV model becomes the SV model (1)-(2) and hence the SV model is a special case of the SR-SV model. We therefore follow the SV literature and assume that $|\phi| < 1$. The z process, and thus the y process of the SR-SV model, is not guaranteed to be stationary unless $\beta_1 = 0$ and $\epsilon_1^\eta \sim \mathcal{N}(\beta_0/(1-\phi), \sigma^2/(1-\phi^2))$. Non-stationarity for volatility is often argued to be more realistic in practice (e.g. van Bellegem (2012)), although it might be mathematically less appealing. The equation in (16) can be further written out as

$$z_t = \beta_0 + \beta_1 \mathfrak{N}(\eta_{t-1}, w_z z_{t-1}, h_{t-1}) + \phi z_{t-1} + \epsilon_t^\eta, \quad (17)$$

where $\mathfrak{N}(\cdot)$ is a non-linear function and w_z is the weight corresponding to z_{t-1} ; see the full version of the SR-SV model in the Appendix. If $w_z = 0$ in (17), then z_t only depends linearly on z_{t-1} , therefore this equation indicates that the parameter w_z characterizes the serial dependence rather than linearity that the previous log volatility z_{t-1} has on z_t . We will analyse w_z in more details in Section 4.

Second, Oliva et al. (2017) set the scales α of the SRU model to several pre-specified values to obtain a vector of summary statistics h_t at different moving average weights. We, however, treat α as a model parameter and learn it from the data. We note that a higher α weighs more on the historical information while a smaller α puts a more weight on the current information. We show later in the empirical study that this parameter α is able to quantify the existence

of the long-memory auto-dependence commonly exhibited in the volatility dynamics of the financial time series.

Third, neural networks are highly flexible but often subject to overfitting, i.e., they have over-confident in-sample fit and bad out-of-sample forecasts. Regularization is often needed to avoid overfitting. Injecting noise into the layers of the network has been found an effective regularization approach in the Machine Learning literature, and seen as a form of data augmentation at multiple levels of abstraction (Sietsma and Dow, 1991; Poole et al., 2014; Goodfellow et al., 2016; Dieng et al., 2018). In the SR-SV model, by allowing z_{t-1} and η_{t-1} to be the inputs of the SRU structure at time t , we inject the noise ϵ_{t-1}^η of the volatility process to the input and hidden layers of the SRU. This noise-injecting regularization approach makes the SR-SV model perform well on both in-sample fitting and out-of-sample forecast, even with the simplest specification of the SRU structure where all the r_t , φ_t and h_t are scalars. Our SR-SV model can be categorized as a *parametric* model with the vector of model parameters θ consisting of eleven parameters: four main parameters β_0 , β_1 , ϕ , σ^2 and the parameters in the SRU including $\alpha, w_h, b_r, w_r, w_\eta, w_z$ and b_φ .

Finally, β_0 plays the role of the scale factor $\tau = e^{\beta_0/2}$ for the variance of y_t . One could set $\beta_0 = 0$ and modify (15) to $y_t = \tau e^{\frac{1}{2}z_t} \epsilon_t^y$; however, this parameterization might be less statistically efficient in terms of Bayesian estimation, especially for the parameter τ (see Kim et al., 1998).

It is straightforward to extend the SR-SV model in (12)-(15) by incorporating other advances in the SV literature. For example, we can use a Student's t distribution instead of a Gaussian for the measurement shock ϵ_t^y and take into account the leverage effect by correlating ϵ_t^y with the volatility shock ϵ_t^η . We do not consider these extensions here, however, because using the most basic version makes it easier to understand the strengths and weaknesses of the new model.

3 Bayesian inference

This section discusses Bayesian estimation and inference for the SR-SV model. For a generic sequence $\{x_t\}$ we use $x_{i:j}$ to denote the series (x_i, \dots, x_j) . The SR-SV model is a state-space model with the measurement equation

$$y_t | z_t \sim \mathcal{N}(0, e^{z_t}), \quad (18)$$

and the state transition equation

$$z_t | z_{1:t-1}, h_t \sim \mathcal{N}(\phi z_{t-1} + \beta_0 + \beta_1 h_t, \sigma^2), \quad t \geq 2, \quad z_1 \sim \mathcal{N}(\beta_0, \sigma^2). \quad (19)$$

We are interested in sampling from the posterior distribution of θ

$$\pi(\theta) = p(\theta | y_{1:T}) = \frac{p(y_{1:T} | \theta) p(\theta)}{p(y_{1:T})}, \quad (20)$$

where $p(y_{1:T} | \theta)$ is the likelihood function, $p(\theta)$ is the prior and $p(y_{1:T}) = \int_{\Theta} p(y_{1:T} | \theta) p(\theta) d\theta$ is the marginal likelihood. Recall that the vector of model parameters θ consists of β_0 , β_1 , ϕ , σ^2 and the 7 parameters within the SRU model (11a)-(11c).

The likelihood function in (20) is

$$p(y_{1:T} | \theta) = \int p(y_{1:T} | z_{1:T}, \theta) p(z_{1:T} | \theta) dz_{1:T}, \quad (21)$$

which is computationally intractable for non-linear non-Gaussian state space models like the SV and SR-SV models, but can be estimated unbiasedly by a particle filter (Del Moral, 2004). Bayesian inference for SR-SV can be performed using recent advances in the Sequential Monte Carlo literature that we present next.

3.1 The Density Tempered Sequential Monte Carlo for the SR-SV model

Duan and Fulop (2015) propose the Density Tempered Sequential Monte Carlo (DT-SMC) approach to Bayesian inference for state space models where the likelihood is intractable. The DT-SMC sampler generalizes the SMC method of Neal (2001) and Del Moral et al. (2006) when the likelihood can be computed analytically. In order to sample from the posterior $\pi(\theta)$, the DT-SMC method first samples a set of M weighted particles $\{W_0^j, \theta_0^j\}_{j=1}^M$ from an easy-to-sample distribution $\pi_0(\theta)$, such as the prior $p(\theta)$, and then traverses these particles through intermediate distributions $\pi_t(\theta)$, $t=1, \dots, K$, which target the posterior distribution $\pi(\theta)$ eventually, i.e. $\pi_K(\theta) = \pi(\theta)$. The DT-SMC method uses the following intermediate distributions

$$\pi_t(\theta) := \pi_t(\theta|y_{1:T}) \propto \hat{p}(y_{1:T}|\theta, u)^{\gamma_t} p(\theta), \quad (22)$$

where the γ_t is referred to as the level temperature and $0 = \gamma_0 < \gamma_1 < \gamma_2 < \dots < \gamma_K = 1$, $\hat{p}(y_{1:T}|\theta, u)$ is the unbiased estimator of the likelihood $p(y_{1:T}|\theta)$ and u is the set of pseudo random numbers used within a particle filter to estimate the likelihood $p(y_{1:T}|\theta)$. For the purpose of this paper where it is possible to sample from the prior $p(\theta)$, we set $\pi_0(\theta) = p(\theta)$. Algorithm 1 summarizes the DT-SMC method for the SR-SV model.

The DT-SMC method consists of three main steps: reweighting, resampling and Markov move. At the beginning of SMC iteration t , the set of weighted particles $\{W_{t-1}^j, \theta_{t-1}^j\}_{j=1}^M$ that approximate the intermediate distribution $\pi_{t-1}(\theta)$ is reweighted to approximate the target $\pi_t(\theta)$. The efficiency of these weighted particles is often measured by the effective sample size (ESS) (Kass et al., 1998; Liu and Chen, 1998) defined in (25). If the ESS is below a prespecified threshold, the particles are resampled; the resulting equally-weighted resamples, which are now approximate samples from $\pi_t(\theta)$, are then refreshed by a Markov kernel whose invariant distribution is $\pi_t(\theta)$. For example, Duan and Fulop (2015) uses the pseudo marginal Metropolis-Hastings (PMMH) kernel of Andrieu et al. (2010) with the likelihood estimated unbiasedly by the particle filter in the Markov move step. However, Pitt et al. (2012) suggest that the PMMH approach works efficiently when the variance of the log of the estimated likelihood is around 1. For some state space models like the SR-SV model, a large number of particles might be required to obtain a likelihood estimator with log variance to be around 1, which is computationally inefficient. To tackle this problem, we incorporate the Correlated Pseudo Marginal (CPM) approach of Deligiannidis et al. (2018) into the Markov move step. The CPM method makes the current set of random numbers u and proposal u' correlated, and helps reduce the variance of the ratio $\hat{p}(y_{1:T}|\theta', u')/\hat{p}(y_{1:T}|\theta, u)$ in (26), thus leading to a better mixing Markov chain while using less number of particles in the particle filter. Similar to the SMC methods of Del Moral et al. (2006) and Neal (2001), the DT-SMC method is parallelizable as the particles move independently in the Markov move step, and provides an estimate of the marginal likelihood as a by-product.

In Algorithm 1, we use a random walk proposal for $q(\theta'|\theta)$. We follow Gunawan et al. (2018) and choose the tempering sequence γ_t adaptively to ensure a sufficient level of particle efficiency by selecting the next value of γ_t such that ESS stays above a threshold.

3.2 Model choice by marginal likelihood

The marginal likelihood is often used to choose between models via the Bayes factor (Jeffreys, 1935; Kass and Raftery, 1995). In order to compare the relative performance between two models M_1 and M_2 on a given data $y_{1:T}$, we can use the Bayes factor defined by

$$F_{M_1, M_2} = \frac{p(y_{1:T}|M_1)}{p(y_{1:T}|M_2)}, \quad (28)$$

providing a Bayesian alternative to hypothesis testing. The larger the Bayes factor F_{M_1, M_2} , the stronger M_1 is supported by the data than M_2 . Jeffreys (1961) suggests a scale of interpretation of the Bayes factor F_{M_1, M_2} as listed in Table 1. We note that the DT-SMC sampler in the previous section provides an efficient way to compute the marginal likelihood.

Grade	F_{M_1, M_2}	$\log_{10} F_{M_1, M_2}$	$\ln F_{M_1, M_2}$	Strength of evidence
0	$< 10^0$	< 0	< 0	Negative (supports M_2)
1	$10^0 - 10^{1/2}$	$0.0 - 0.5$	$0.0 - 1.2$	Barely worth mentioning
2	$10^{1/2} - 10^1$	$0.5 - 1.0$	$1.2 - 2.3$	Substantial
3	$10^1 - 10^{3/2}$	$1.0 - 1.5$	$2.3 - 3.5$	Strong
4	$10^{3/2} - 10^2$	$1.5 - 2.0$	$3.5 - 4.6$	Very strong
5	$> 10^2$	> 2.0	> 4.6	Decisive

Table 1: Jeffreys’ scale of interpretation of the Bayes Factor F_{M_1, M_2} .

4 Simulation studies and applications

This section evaluates the performance of the SR-SV model relative to the SV, N-SV and LMSV models using a simulation study and real data applications. We do not report the results for GARCH as it performs similarly to SV. We use the DT-SMC sampler for the Bayesian inference in the SV, N-SV and SR-SV models. As the LMSV model does not have an explicit state-space representation and its likelihood function is analytically intractable, we follow Breidt et al. (1998) and estimate the LMSV model on the frequency domain. The implementation of Bayesian inference for the LMSV model is presented in Appendix A.1. Table 14 in Appendix A.3 lists our implementation details of the DT-SMC sampler. All the computations are run on a High-Performance Computing (HPC) machine with 16-core CPU and 16 Gigabytes of RAM. The DT-SMC sampler was initialized by sampling from the priors in Table 2.

We now motivate the choice of the priors in Table 2. We follow Yu et al. (2006) and Kim et al. (1998) to set the same prior, which is a Beta distribution, for the persistence parameters

Algorithm 1 The Density Tempered Sequential Monte Carlo for the SR-SV model

1. Sample $\theta_0^j \sim p(\theta)$, $u_0^j \sim p(u)$ and set $W_0^j = 1/M$ for $j = 1 \dots M$
2. **For** $t = 1, \dots, K$,

Step 1: Reweighting: Compute the unnormalized weights

$$w_t^j = W_{t-1}^j \frac{\widehat{p}(y_{1:T}|\theta_{t-1}^j, u_{t-1}^j)^{\gamma_t} p(\theta_{t-1}^j)}{\widehat{p}(y_{1:T}|\theta_{t-1}^j, u_{t-1}^j)^{\gamma_{t-1}} p(\theta_{t-1}^j)} = W_{t-1}^j \widehat{p}(y_{1:T}|\theta_{t-1}^j, u_{t-1}^j)^{\gamma_t - \gamma_{t-1}}, \quad j = 1, \dots, M \quad (23)$$

and set the new normalized weights

$$W_t^j = \frac{w_t^j}{\sum_{s=1}^M w_t^s}, \quad j = 1, \dots, M. \quad (24)$$

Step 2: Compute the effective sample size (ESS):

$$\text{ESS} = \frac{1}{\sum_{j=1}^M (W_t^j)^2}. \quad (25)$$

if $\text{ESS} < cM$ for some $0 < c < 1$, **then**

- (i) **Resampling:** Resampling from $\{\theta_{t-1}^j, u_{t-1}^j\}_{j=1}^M$ using the weights $\{W_t^j\}_{j=1}^M$, and then set $W_t^j = 1/M$ for $j = 1 \dots M$, to obtain the new equally-weighted particles $\{\theta_t^j, u_t^j, W_t^j\}_{j=1}^M$.
- (ii) **Markov move:** For each $j = 1, \dots, M$, move the samples θ_t^j, u_t^j according to N_{CPM} CPM steps:
 - (a) Sample $\theta_t^{j'}$ from the proposal density $q(\theta_t^{j'}|\theta_t^j)$.
 - (b) Sample $\epsilon^j \sim \mathcal{N}(0_D, I_D)$ and set $u_t^{j'} = \rho u_t^j + \sqrt{1 - \rho^2} \epsilon^j$ with $\rho \in (-1, 1)$ is a correlation factor.
 - (c) Compute the estimated likelihood $\widehat{p}(y_{1:T}|\theta_t^{j'}, u_t^{j'})$ using a particle filter (see Algorithm 3 in Appendix A.3)
 - (d) Set $\theta_t^j = \theta_t^{j'}$ and $u_t^j = u_t^{j'}$ with the probability

$$\min \left(1, \frac{\widehat{p}(y_{1:T}|\theta_t^{j'}, u_t^{j'})^{\gamma_t} p(\theta_t^{j'})}{\widehat{p}(y_{1:T}|\theta_t^j, u_t^j)^{\gamma_t} p(\theta_t^j)} \frac{q(\theta_t^j|\theta_t^{j'})}{q(\theta_t^{j'}|\theta_t^j)} \right), \quad (26)$$

otherwise keep θ_t^j, u_t^j unchanged.

end

3. The log of marginal likelihood estimate is

$$\log \widehat{p}(y_{1:T}) = \sum_{t=1}^K \log \left(\sum_{j=1}^M w_t^j \right). \quad (27)$$

SR-SV		SV		N-SV	
Parameter	Prior	Parameter	Prior	Parameter	Prior
β_0	$\mathcal{N}(0,0.1)$	μ	$\mathcal{N}(0,25)$	μ	$\mathcal{N}(0,25)$
$\frac{\phi+1}{2}$	Beta(20,1.5)	$\frac{\phi+1}{2}$	Beta(20,1.5)	$\frac{\phi+1}{2}$	Beta(20,1.5)
σ^2	$IG(2.5,0.25)$	σ^2	$IG(2.5,0.25)$	σ^2	$IG(2.5,0.25)$
β_1	$IG(2.5,1)$			δ	$\mathcal{N}(0,0.1)$
α	Beta(2,2)				
w_h, w_ϕ, w_η	$\mathcal{N}(0,0.1)$				
b_r, b_ϕ	$\mathcal{N}(0,0.1)$				
w_z	$IG(2.5,1)$				

Table 2: Prior distributions for the parameters in the SR-SV, SV and N-SV models. The notation \mathcal{N} , IG and Beta denote the Gaussian, inverse-Gamma and Beta distributions, respectively.

ϕ of the three models SV, N-SV and SR-SV. We also use an inverse-Gamma prior for the parameters σ^2 in all models but make it more flat than the priors used in Yu et al. (2006) and Kim et al. (1998). We follow Yu et al. (2006) to use an informative but reasonably flat prior distribution for the intercept μ in the SV and N-SV models. For the SR-SV model, we found that the posterior distributions of β_1 and w_z to be unimodal under inverse-Gamma priors. We use a normal prior with a zero mean and a small variance for the SRU parameters, except w_z , because empirical results from the SRU literature show that the values of the SRU parameters are often small. Finally, we set a normal prior with a zero mean and a small variance for the intercept β_0 in the SR-SV model as the empirical results often show small values of β_0 .

Table 3 lists the predictive scores used to measure the out-of-sample performance. The smaller the predictive scores, the better.

Score	Definition	Score	Definition
PPS	$-T_{test}^{-1} \sum_{D_{test}} \log p(y_t y_{1:t-1}, \hat{\theta})$	MSE ₁	$T_{test}^{-1} \sum_{D_{test}} (\sigma_t - \hat{\sigma}_t)^2$
QLIKE	$T_{test}^{-1} \sum_{D_{test}} (\log(\hat{\sigma}_t^2) + \sigma_t^2 \hat{\sigma}_t^{-2})$	MSE ₂	$T_{test}^{-1} \sum_{D_{test}} (\sigma_t^2 - \hat{\sigma}_t^2)^2$
R ² LOG	$T_{test}^{-1} \sum_{D_{test}} [\log(\sigma_t^2 \hat{\sigma}_t^{-2})]^2$	MAE ₁	$T_{test}^{-1} \sum_{D_{test}} \sigma_t - \hat{\sigma}_t $
		MAE ₂	$T_{test}^{-1} \sum_{D_{test}} \sigma_t^2 - \hat{\sigma}_t^2 $

Table 3: Definition of the predictive scores to measure the out-of-sample performance on simulation and real index data. Here, $\hat{\sigma}_t$ is an estimate of the volatility σ_t , T_{test} is the number of observations in test data D_{test} and $\hat{\theta}$ is a posterior mean estimate of θ .

4.1 Simulation studies

We consider three volatility models specified in Table 4. Model 1 is a GARCH(1,1). Model 2 is an extension of the GARCH(1,1) model by applying a Box-Cox power transformation (Box and Cox, 1964) to both the conditional variance equation and the volatility dynamics. Model 3 is similar to the non-linear ARCH models of Higgins and Bera (1992) but they use lagged innovations to construct the conditional variance. Model 3 is a FIGARCH(1, d ,1) model of Baillie et al. (1996) which uses a long-memory process AFRIMA(1, d ,1) to simulate the long-memory auto-dependence.

Data	Model	Parameters
SIM I	$\sigma_t^2 = \mu + \alpha y_{t-1}^2 + \beta \sigma_{t-1}^2, \quad t = 2, \dots, T$ $y_t = \sigma_t \epsilon_t, \quad \epsilon_t \sim \mathcal{N}(0,1), \quad t = 1, \dots, T$	$\sigma_1^2 = 0.1, \quad \mu = 0.1$ $\alpha = 0.07, \quad \beta = 0.92$
SIM II	$h_t = \mu + \alpha \frac{(y_{t-1}^2)^\delta - 1}{\delta} + \beta h_{t-1}, \quad t = 2, \dots, T$ $y_t = \left(1 + \delta h_t\right)^{1/2\delta} \epsilon_t, \quad \epsilon_t \sim \mathcal{N}(0,1), \quad t = 1, \dots, T$	$h_1 = 0.1, \quad \mu = 0.1$ $\alpha = 0.15, \quad \beta = 0.82$ $\delta = 0.9$
SIM III	$\sigma_t^2 = \mu + \left[1 - \beta B - (1 - \phi B)(1 - B)^d\right] y_t^2 + \beta \sigma_{t-1}^2, \quad t = 2, \dots, T$ $y_t = \sigma_t \epsilon_t, \quad \epsilon_t \sim \mathcal{N}(0,1), \quad t = 1, \dots, T$	$\sigma_1^2 = 0.1, \quad \mu = 0.01$ $\phi = 0.01, \quad \beta = 0.5$ $d = 0.62$

Table 4: Simulation: Data generating process.

We generate time series of $T = 3000$ observations from these three models and name the simulation datasets as SIM I, SIM II, SIM III, accordingly. The parameters are set so that y_t somewhat resembles real financial time series data exhibiting volatility clustering with non-linearity (SIM II) and long-memory (SIM III) auto-dependence in the underlying volatility dynamics. For each dataset, the first $T_{in} = 2000$ observations are used for model estimation and the last $T_{out} = 1000$ are for out-of-sample analysis. Table 5 shows the posterior mean estimates for the parameters of the SV and SR-SV models, with the posterior standard deviations in brackets; for the SR-SV model we only show the results for the main parameters. The last column in the table shows the marginal likelihood estimates, averaged over 10 different runs of the DT-SMC sampler, together with the Monte Carlo standard errors in the brackets. Figures 4, 5 and 6 plot the filtered values of the η_t and h_t components of the SR-SV model in SIM I, SIM II and SIM III datasets, respectively. Figure 12 in Appendix A.4 plots the true volatility together with the filtered volatility produced by the SV and SR-SV models, for all the three simulation datasets.

	μ	ϕ	σ^2	α	β_0	β_1	w_z	Mar.llh
SIM I								
SV	2.145 (0.237)	0.985 (0.004)	0.019 (0.003)					−5100.8 (0.131)
SR-SV		0.974 (0.023)	0.020 (0.005)	0.534 (0.166)	0.027 (0.031)	0.388 (0.235)	−0.205 (0.261)	−5099.9 (0.300)
SIM II								
SV	1.050 (0.125)	0.967 (0.008)	0.032 (0.006)					−4060.3 (0.164)
SR-SV		0.792 (0.106)	0.041 (0.010)	0.515 (0.156)	0.043 (0.044)	0.423 (0.207)	0.530 (0.256)	−4057.7* (0.306)
SIM III								
SV	0.134 (0.329)	0.984 (0.005)	0.041 (0.007)					−3146.9 (0.195)
SR-SV		0.896 (0.035)	0.056 (0.013)	0.645 (0.240)	−0.093 (0.045)	0.325 (0.132)	0.290 (0.115)	−3144.2* (0.316)

Table 5: Simulation: Posterior means of the parameters with the posterior standard deviations in brackets. The last column shows the estimated log marginal likelihood with the Monte Carlo standard errors in brackets, averaged over 10 different runs of the DT-SMC sampler. The asterisks indicate the cases when the Bayes factors strongly support the SR-SV model over the SV model. The marginal likelihood are reported in natural log scale.

The estimation results suggest the following conclusions. First, for the SIM I data, the difference of marginal likelihood estimates in Table 5 between the SV and SR-SV models is insignificant, the coefficient β_1 is insignificant, and the filtered volatilities from these two models in Figure 12 are identical and close to the true volatility. This implies that the SV and SR-SV models fit equally well to the SIM I data and that the SR-SV model is close to the SV model if the true data generating process, which is GARCH(1,1) in this example, exhibits no other effects rather than short-memory linear auto-dependence within the volatility dynamics.

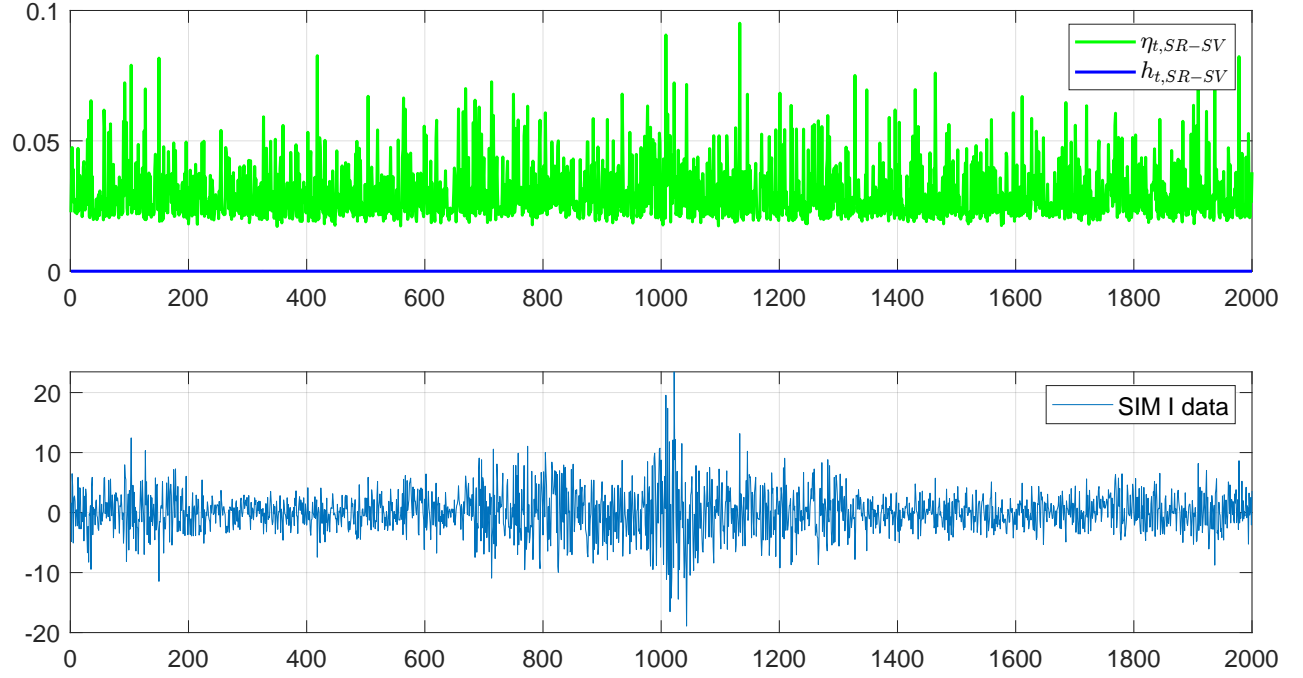


Figure 4: SIM I: The filtered values of η_t and h_t of the SR-SV model, together with the SIM I in-sample data. (This is better viewed in colour).

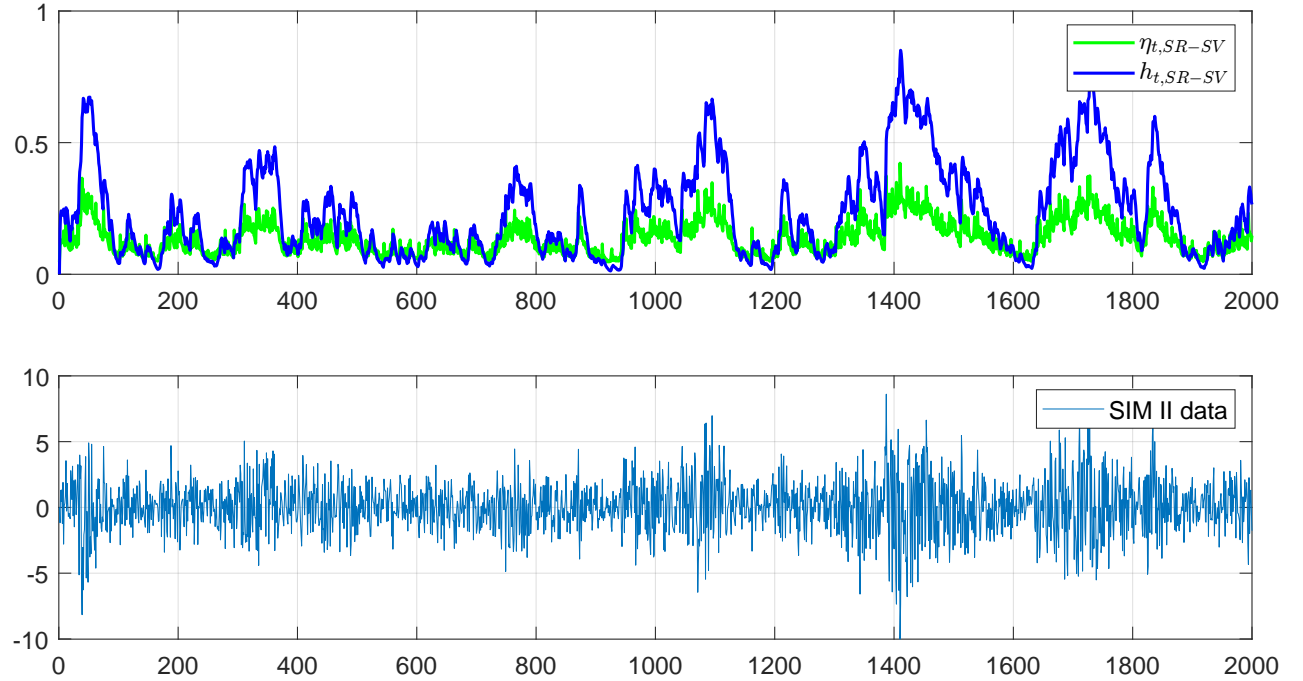


Figure 5: SIM II: The filtered values of η_t and h_t of the SR-SV model, together with the SIM II in-sample data. (This is better viewed in colour).

Second, the estimation results on the SIM II and SIM III data show that the additional neural network structure of the SR-SV model is able to efficiently capture the volatility effects

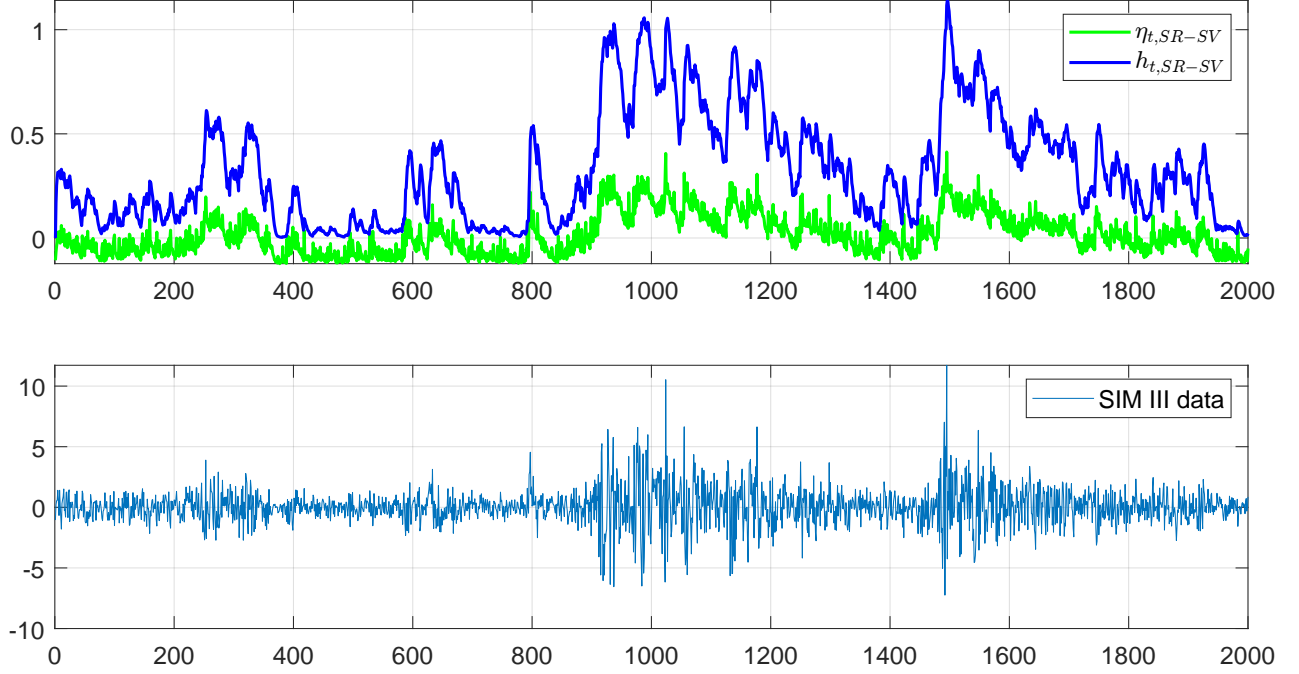


Figure 6: SIM III: The filtered values of η_t and h_t of the SR-SV model, together with the SIM III in-sample data. (This is better viewed in colour).

overlooked by the basic SV model. This is supported by the Bayes factors of the SR-SV model compared to the SV model of more than $e^{2.3}$, which, according to the interpretation in Table 1, strongly support the SR-SV model. The plots of the h_t and η_t components of the SR-SV model in Figures 4, 5 and 6 clearly show that h_t , and hence η_t , is well responsive to volatility effects rather than the linear short-memory effects. For example, in the SIM I data when the volatility exhibits no non-linear and long-memory effects, the h_t shown in Figure 4 is significantly small at all time steps and hence the η_t component simply fluctuates around β_0 during both low and high volatility periods. Figures 5 and 6, on the other hand, show that the h_t response adaptively to the changes in the volatility dynamics. As the result, η_t is small during the low volatility periods and large in the high volatility periods. The non-linear (SIM II) and long-memory (SIM III) auto-dependence of the simulated volatility are well captured by the SRU structure of the SR-SV model. The plots of filtered volatility in Figure 12 show that the filtered volatility of the SR-SV model are generally closer to the true volatility than those of the SV model.

Third, the parameters of the SR-SV model are able to characterize well the existence of the various volatility effects in these simulation data. The estimated posterior means of parameter β_1 are more than two standard deviations from zero in the SIM II and SIM III data, suggesting the existence of volatility effects rather than linearity in the volatility dynamics of these two datasets; while β_1 is less than two standard deviations from zero in the SIM I data, suggesting that only simple linear effects are detectable in the volatility dynamics of this dataset. Similarly, the non-linear coefficient w_z of the SR-SV model (c.f. equation (17)) is more than two standard deviations from zero in the SIM II and SIM III data but not in the SIM I data, indicating that the SR-SV model is able to detect the serial dependence rather than the linear dependence that the past log volatility z_{t-1} has on the current log volatility

z_t . The estimated posterior mean of the moving average weight parameter α in the SIM III data is higher than those in the SIM I and SIM II data, supporting further the evidence of the long-memory auto-dependence exhibited in the volatility dynamic of the SIM III data, which is generated from a FIGARCH(1, d ,1) model. Figure 7 shows that the posterior mode of α in the SIM III data is much closer to 1 than those in the SIM I and SIM II data. Finally, it is worth noting that the persistence parameter ϕ of the SR-SV is close to the persistence parameter ϕ of the SV model in the SIM I data but much smaller than that of the SV model in the SIM II and SIM III model. This is probably because the non-linear coefficient w_z with respect to the past log volatility z_{t-1} is significant in the SIM II and SIM III data, and hence the historical information has been also well stored in the η_t process.

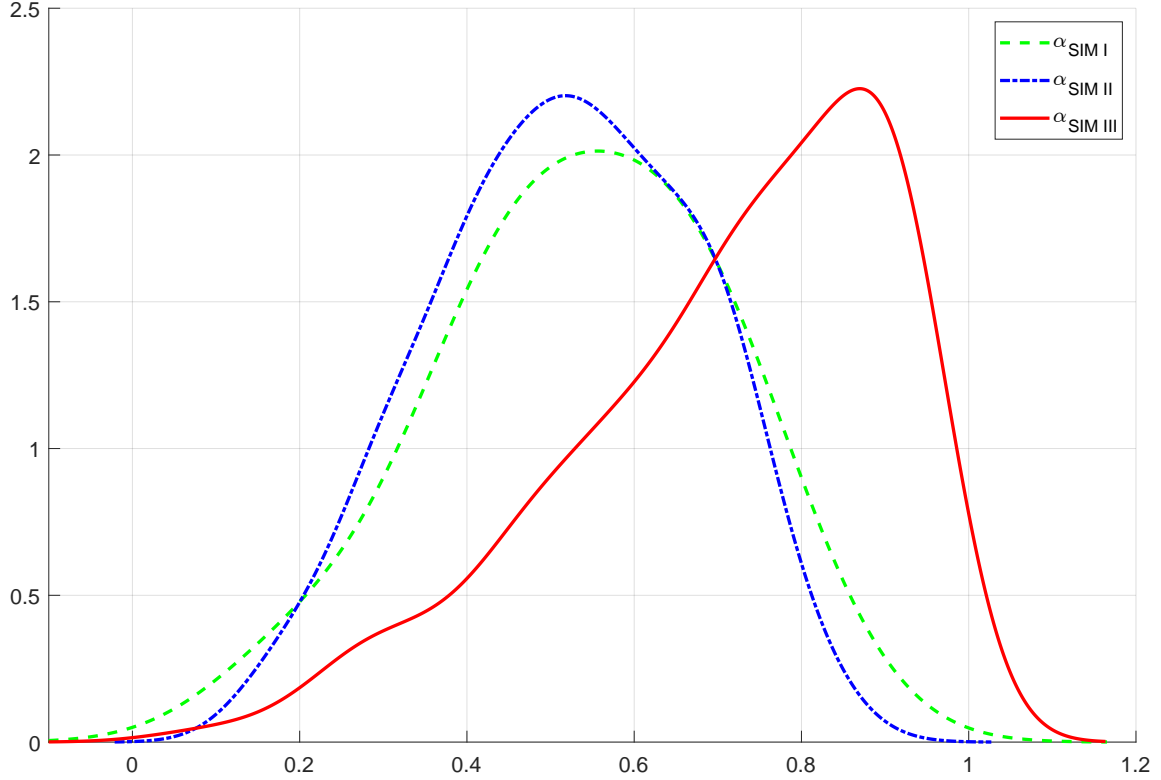


Figure 7: Simulation: Posterior densities of the moving average weight α on the three simulation datasets.

	PPS	MSE ₁	MSE ₂	MAE ₁	MAE ₂	QLIKE	R ² LOG	Count
SIM I								
SV	2.355 (0.001)	0.480 (0.003)	0.485 (0.003)	0.506 (0.002)	0.540 (0.004)	0.481 (0.001)	0.482 (0.004)	1
SR-SV	2.357 (0.000)	0.435 (0.002)	0.381 (0.003)	0.342 (0.001)	0.319 (0.002)	0.450 (0.001)	0.395 (0.003)	6
SIM II								
SV	1.881 (0.000)	0.189 (0.000)	0.282 (0.001)	0.309 (0.001)	0.383 (0.001)	0.359 (0.001)	0.512 (0.001)	0
SR-SV	1.878 (0.000)	0.076 (0.002)	0.122 (0.003)	0.139 (0.002)	0.189 (0.000)	0.172 (0.003)	0.284 (0.003)	7
SIM III								
SV	1.722 (0.001)	0.919 (0.004)	0.967 (0.004)	0.707 (0.003)	0.796 (0.003)	0.754 (0.004)	0.529 (0.004)	0
SR-SV	1.720 (0.000)	0.733 (0.004)	0.775 (0.003)	0.548 (0.002)	0.625 (0.003)	0.588 (0.003)	0.399 (0.002)	7

Table 6: Simulation: Forecast performance of the SR-SV and SV models. In each panel, the bold numbers indicate the best predictive scores and the count indicates the number of times a model has better forecast scores than the other one. Monte Carlo standard errors in brackets, averaged over 10 different runs.

Table 6 reports the predictive performance scores of the SV and SR-SV models with the Monte Carlo standard errors in brackets. For the SIM II and SIM III data, the SR-SV model outperforms the SV model for all the predictive scores, which is consistent with the in-sample analysis showing that the SR-SV model fits these simulation datasets better than the SV model. For the SIM I data, the SR-SV model also outperforms the SV model for all scores except the PPS score. These results illustrate the impressive out-of-sample forecast ability of the SR-SV model. The results for the real data applications in the next section further support this claim.

4.2 Applications

This section evaluates the SR-SV model using five popular daily stock indexes from different international markets: The German stock index DAX30 (DAX), the Hong Kong stock index HS50 (HSI), the France market index CAC40 (FCHI), the US stock market index SP500 (SPX) and the Canada market index TSX250 (TSX).

4.2.1 The datasets and exploratory data analysis

The datasets were downloaded from the Realized Library of The Oxford-Man Institute². We used the adjusted closing prices $\{P_t, t=1, \dots, T_P\}$ and calculated the demeaned return process

²<https://realized.oxford-man.ox.ac.uk/>

as

$$y_t = 100 \left(\log \frac{P_{t+1}}{P_t} - \frac{1}{T_P - 1} \sum_{i=1}^{T_P-1} \log \frac{P_{i+1}}{P_i} \right), \quad t = 1, 2, \dots, T_P - 1, \quad (29)$$

and using the first $T_{\text{in}} = 2000$ returns for in-sample analysis and the rest $T_{\text{out}} = 1000$ for out-of-sample analysis. Table 7 describes the relevant aspects of the datasets.

	In-sample Period	Out-of-sample Period	T_{in}	T_{out}
DAX	23 Apr 2004 – 21 Feb 2012	22 Feb 2012 – 05 Feb 2016	2000	1000
HSI	27 Oct 2003 – 28 Nov 2011	29 Nov 2011 – 21 Dec 2015	2000	1000
FCHI	09 Jun 2004 – 22 Mar 2012	23 Mar 2012 – 23 Feb 2016	2000	1000
SPX	27 Feb 2004 – 06 Feb 2012	07 Feb 2012 – 28 Jan 2016	2000	1000
TSX	03 Feb 2004 – 01 Feb 2012	02 Feb 2012 – 27 Jan 2016	2000	1000

Table 7: Descriptions of the five index datasets.

	Min	Max	Std	Skew	Kurtosis	$V_n(10)$	$V_n(20)$	$V_n(30)$
DAX	-7.437	9.993	1.267	0.115	10.960	3.226*	2.501*	2.146*
						2.456*	1.926*	1.670
HSI	-11.616	12.155	1.186	0.307	17.551	3.934*	3.030*	2.587*
						2.564*	2.088*	1.844*
FCHI	-7.215	6.663	1.132	-0.320	7.383	3.782*	2.976*	2.575*
						3.018*	2.453*	2.165*
SPX	-9.351	10.220	1.307	-0.256	12.502	3.188*	2.412*	2.047*
						2.664*	2.040*	1.748*
TSX	-9.879	9.194	1.262	-0.727	12.202	3.558*	2.692*	2.277*
						2.877*	2.199*	1.875*

Table 8: Descriptive statistics for the demeaned returns of the DAX, HSI, FCHI, SPX and TSX datasets. $V_n(q)$, $q = 10, 20$ and 30 , shows the test statistics of Lo’s modified R/S test of long memory with lag q . Upper and lower values of the 3 last columns are the Lo’s test statistics for absolute and squared returns, respectively. The asterisks indicate significance at the 5% level.

Figure 11 in Appendix A.4 plots the time series data and shows the existence of the volatility clustering effect commonly seen in financial data. Table 8 reports some descriptive statistics together with Lo’s modified R/S test (Lo, 1991) for long-range memory in the absolute and squared returns. Lo’s modified R/S test is widely used in the financial time series literature; see, e.g., Lo (1991), Giraitis et al. (2003), Breidt et al. (1998). All the index data exhibit some negative skewness, high excess kurtosis and high variation. The result of Lo’s

modified R/S test for long-memory dependence with several different lags q indicates that there is significant evidence of long-memory dependence in the stock indices.

The Realized Library provides different realized measures³ that can be used in financial econometrics as a proxy to the latent σ_t^2 . We use the following four common realized measures including Realized Variance (RV) (Andersen and Bollerslev, 1998), Bipower Variation (BV) (Barndorff-Nielsen and Shephard, 2004), Median Realized Volatility (MedRV) (Andersen et al., 2012), Realized Kernel Variance (Barndorff-Nielsen et al., 2008) with the Non-Flat Parzen kernel (RKV) to evaluate the forecast performance of the volatility models using the predictive scores in Table 3. See Shephard and Sheppard (2010) for more details about the Realized Library.

Denote by RV_t the realized measure of σ_t^2 at time t . As the realized measures ignore the variation of the prices overnight and sometimes the variation in the first few minutes of the trading day when recorded prices may contain large errors (Shephard and Sheppard, 2010), we follow Hansen and Lunde (2005) to scale the realized measure RV_t as

$$\tilde{\sigma}_t^2 = \hat{c} \cdot RV_t \text{ where } \hat{c} = \frac{T_{\text{out}}^{-1} \sum_{t=T_{\text{in}}+1}^T (y_t - E(y_t))^2}{T_{\text{out}}^{-1} \sum_{t=T_{\text{in}}+1}^T RV_t}, \quad t = T_{\text{in}} + 1, 2, \dots, T, \quad (30)$$

and use $\tilde{\sigma}_t^2$ as the estimate of the latent conditional variance σ_t^2 . See Table 7 for T_{in} and T_{out} used in our datasets. See Martens (2002) and Fleming et al. (2003) for the similar scaling estimator of the daily volatility.

4.2.2 In-sample analysis

Table 9 summarizes the estimation results of fitting the SV, N-SV and SR-SV models to the five datasets. Table 13 in Appendix A.4 shows the estimation results for the LMSV model. For the SR-SV model, we only show the results of the key parameters. Figure 8 shows the posterior densities of the moving average weight parameter α of the SR-SV model in all simulation and real datasets. We draw some conclusions from Table 9 and the listed figures.

³See <https://realized.oxford-man.ox.ac.uk/documentation/estimators> for the list of the available realized measures

	μ	ϕ	σ^2	δ	α	β_0	β_1	w_z	Mar.llh
DAX									
SV	-0.098 (0.233)	0.979 (0.006)	0.038 (0.008)						-2871.3 (0.171)
N-SV	-0.138 (0.212)	0.977 (0.006)	0.037 (0.008)	-0.198 (0.086)					-2872.4 (0.224)
SR-SV		0.863 (0.052)	0.064 (0.021)		0.605 (0.204)	-0.117 (0.061)	0.410 (0.201)	0.397 (0.153)	-2868.8* (0.301)
HSI									
SV	-0.205 (0.320)	0.987 (0.004)	0.022 (0.008)						-2692.0 (0.184)
N-SV	-0.366 (0.270)	0.987 (0.004)	0.021 (0.004)	-0.242 (0.081)					-2691.0 (0.214)
SR-SV		0.824 (0.061)	0.054 (0.021)		0.784 (0.137)	-0.196 (0.083)	0.536 (0.262)	0.387 (0.139)	-2687.8** (0.337)
FCHI									
SV	-0.213 (0.230)	0.977 (0.007)	0.047 (0.010)						-2787.1 (0.225)
N-SV	-0.217 (0.257)	0.979 (0.006)	0.041 (0.009)	-0.198 (0.089)					-2787.3 (0.234)
SR-SV		0.843 (0.049)	0.093 (0.027)		0.780 (0.197)	-0.179 (0.070)	0.449 (0.199)	0.363 (0.134)	-2784.2* (0.326)
SPX									
SV	-0.228 (0.344)	0.985 (0.005)	0.034 (0.006)						-2748.3 (0.201)
N-SV	-0.267 (0.268)	0.9837 (0.004)	0.036 (0.007)	-0.121 (0.080)					-2749.4 (0.211)
SR-SV		0.844 (0.060)	0.056 (0.017)		0.527 (0.186)	-0.180 (0.186)	0.481 (0.241)	0.373 (0.132)	-2745.6* (0.311)
TSX									
SV	-0.200 (0.323)	0.985 (0.004)	0.028 (0.006)						-2770.1 (0.231)
N-SV	-0.249 (0.298)	0.984 (0.005)	0.029 (0.006)	-0.141 (0.077)					-2769.9 (0.245)
SR-SV		0.868 (0.056)	0.051 (0.015)		0.697 (0.195)	-0.129 (0.071)	0.414 (0.201)	0.355 (0.141)	-2767.2* (0.347)

Table 9: Applications: Posterior means of the parameters with the posterior standard deviations in brackets. The last column shows the estimated log marginal likelihood with the Monte Carlo standard errors in brackets, averaged over 10 different runs of the DT-SMC sampler. The single and double asterisks indicate the cases when the Bayes factors strongly and very strongly support the SR-SV model over the SV model, respectively. The marginal likelihood are reported in natural log scale.

First, the marginal likelihood estimates show that the SR-SV model fits the five index data

better than the SV and N-SV models. The Bayes factors of the SR-SV model compared to the SV and N-SV models are more than $e^{2.3}$, which strongly support the SR-SV in all cases. There are no significant differences between the SV and N-SV models in terms of marginal likelihood estimates across the five panels.

Second, the evidence of the volatility effects rather than linearity, e.g. non-linearity and long-memory auto-dependence, in the volatility dynamics of the index datasets is clear as the posterior means of the non-linearity long-memory parameter β_1 of the SR-SV model are more than two standard deviations from zero in all cases. The estimation results of the LMSV in Table 13 show that the posterior means of the fractional integration parameter d are also more than two standard deviations from zero and close to 0.5 in all cases, suggesting a strong evidence of the long-memory dependence in the volatility process of these five index datasets. The posterior means of the non-linear parameter w_z with respect to the past log volatility z_{t-1} are more than two standard deviations from zero, indicating the existence of the serial dependence rather than linearity that the past log volatility z_{t-1} has on the current log volatility z_t , and that the SR-SV model is able to detect this serial dependence. The posterior density plots of parameter α in Figure 8 suggest the existence of the long-memory auto-dependence in the volatility processes of the index datasets as the posterior densities of α are highly skewed for all cases and the posterior modes are close to 1, which is similar to the results in the SIM III data.

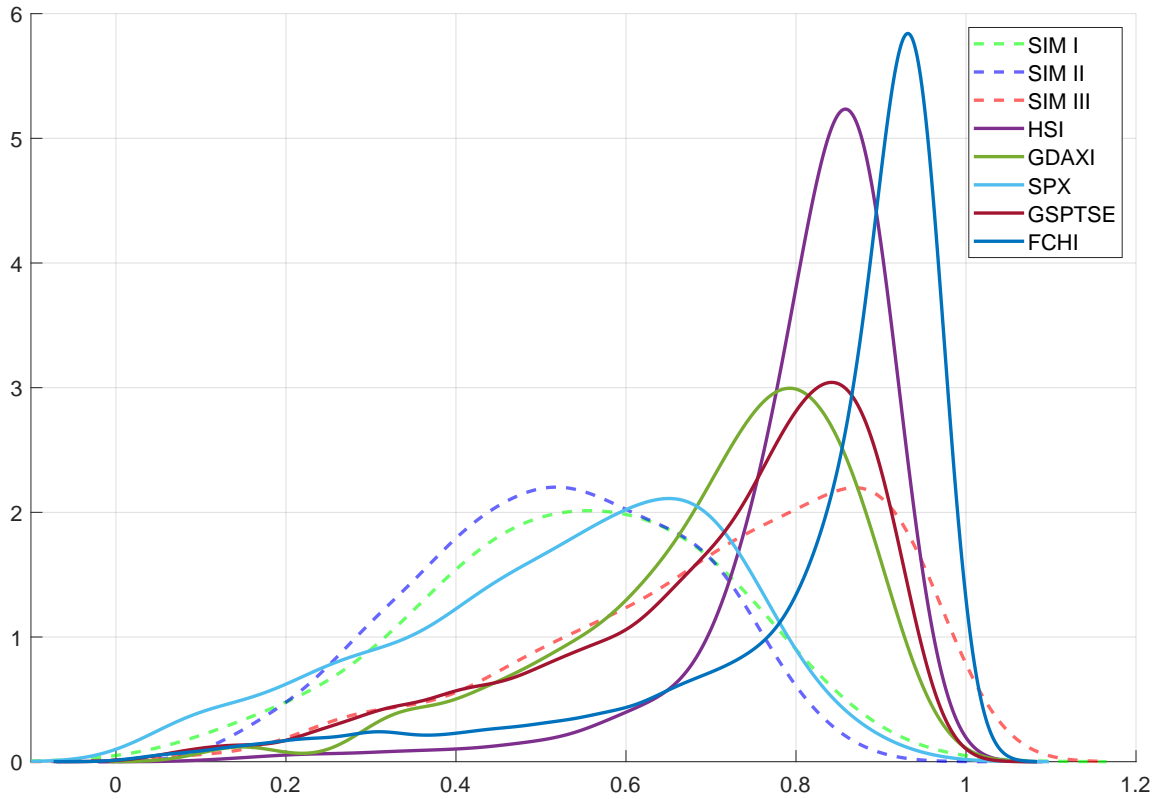


Figure 8: Posterior densities of the moving average weight α on simulation and real datasets. (This is better viewed in colour).

Third, it is worth noting that, in all cases, the persistence parameter ϕ in the SR-SV model is smaller than the persistence parameters in the SV and N-SV models as the parameter w_z

is significant and hence the linear effect that z_{t-1} has on z_t is reduced. As illustrated in the SIM I data, if the volatility process exhibits no volatility effects rather than a short-memory linear auto-dependence, the persistence parameters ϕ in the SV and SR-SV model are similar and the parameter w_z is insignificant.

Using the posterior mean estimates in Table 9, the *filtered* values of z_t of the SR-SV, SV and N-SV models can be computed using the particle filter. We discuss how to obtain the filtered values of z_t of the LMSV model in Appendix A.1. Figure 9 plots the filtered log volatility of the SV and SR-SV model, together with the filtered values of the components h_t and η_t of the SR-SV model in all time steps, for the SPX data. Figure 14, 13, 15 and 16 in Appendix A.4 show the similar plots for the HSI, DAX, FCHI and TSX data, respectively. Figure 9 shows that the component h_t , and hence η_t , of the SR-SV model is well responsive to changes in the volatility dynamics, e.g. being small during the low volatility periods and large in the high volatility periods of the SPX data. The SRU structure of the SR-SV model is able to capture these distinct behaviors of financial time series. We observe the similar behaviors of the h_t and η_t components for the other datasets as shown in the Figures 13-16.

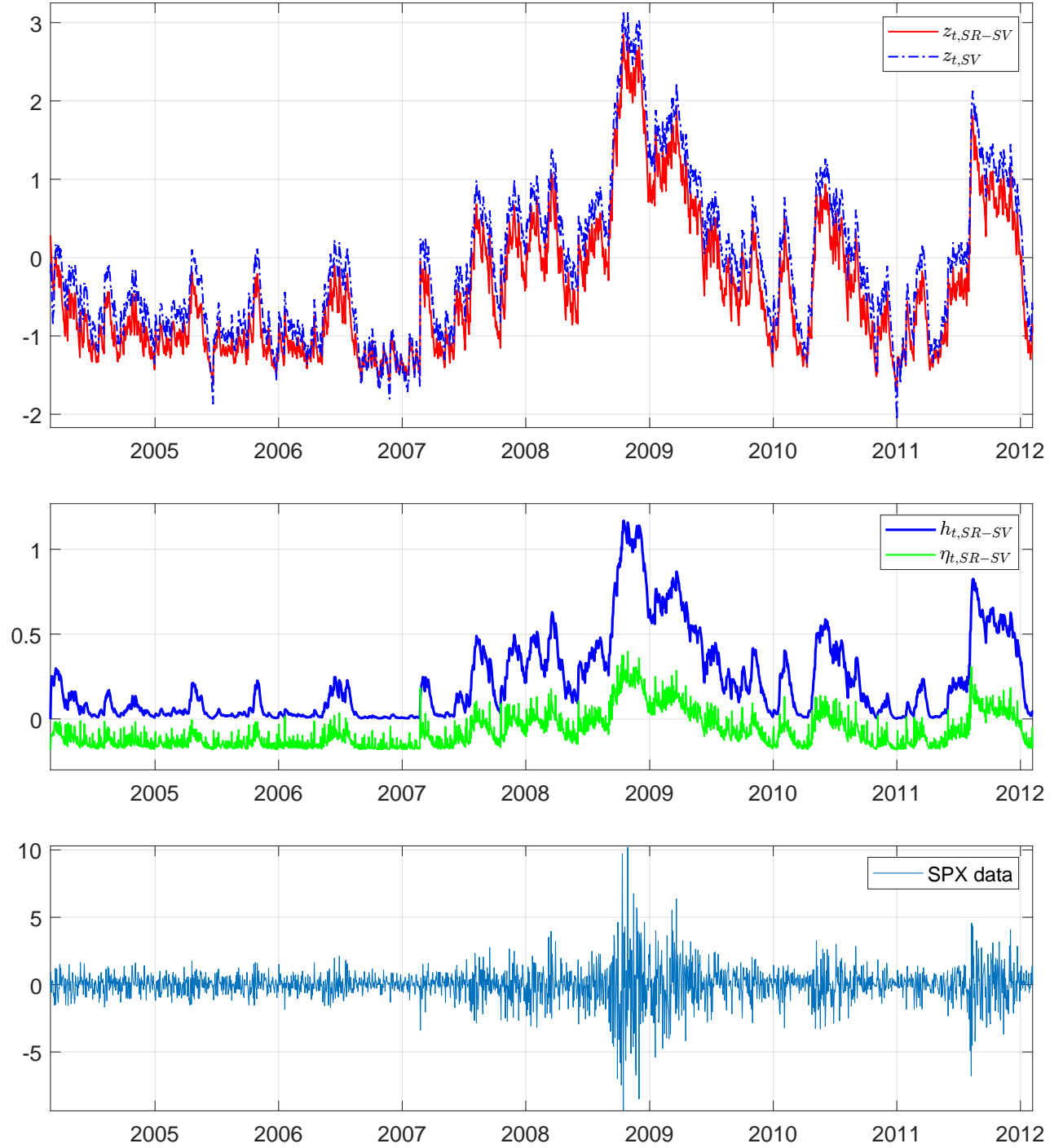


Figure 9: SPX: (*Top*) The filtered log volatility of the SR-SV and SV models. (*Middle*) The filtered values of η_t and h_t of the SR-SV model. (*Bottom*) The SPX in-sample data. (This is better viewed in colour).

Table 10 provides summary statistics on the in-sample filtered volatilities and residuals $\hat{\epsilon}_t^y$ of the SR-SV, SV, N-SV and LMSV models. We note that if the assumption about the normality of returns of the three models is justified then the residuals $\hat{\epsilon}_t^y$ should have a zero skewness and a kurtosis of 3. Table 10 shows that all the residual distributions produced

from the four models are close to the standard normal distribution, but still slightly skewed and leptokurtic. The p -values of the Ljung-Box (LB) autocorrelation test of the residuals are high in all index datasets, suggesting that there is no evidence of autocorrelation in the residuals. We conjecture that extending the SR-SV model, for example, by using a Student's t distribution instead of a Gaussian for the measurement shock ϵ_t^y and taking into account the leverage effect by correlating ϵ_t^y with the volatility shock ϵ_t^η , is likely to lead to better diagnostics for the residuals. However, we do not consider these extensions here.

Out-of-sample analysis

The marginal likelihood estimates in Table 9 suggest that the SR-SV model fits the in-sample data of the five index datasets better than the SV and N-SV models. We now examine if this in-sample performance is consistent with the out-of-sample performance. Table 11 provides summary statistics on the one-step-ahead forecasts of volatility and standardized residuals of the SR-SV, SV, N-SV and LMSV models. We note two conclusions from Table 11.

First, the SR-SV model does not suffer from overfitting as often observed in neural network based volatility models (Pagan and Schwert, 1990; Donaldson and Kamstra, 1997), as the one-step-ahead forecast volatilities and the forecast residuals appear to be well behaved, compared to those from the more parsimonious SV and N-SV models. We emphasize that, as discussed in Section 2.3, the use of noise-injecting regularization in the novel structure of the SR-SV model helps prevent it from the well-known overfitting problem.

Second, the means and standard deviations of one-step-ahead forecast volatility of the SR-SV model are smaller than those of the SV, N-SV and LMSV in all five index datasets. The SR-SV forecasts are generally more conservative in low volatility periods, in the sense that the forecast intervals often have a smaller band compared to the forecasts produced by the other models. The comparison of 99% one-step-ahead forecast intervals during the period Sep 2014 - May 2015 of the SPX data in Figure 10 shows that the SR-SV model gives a safe buffer against abrupt changes in low volatility regions, e.g. Nov-Dec 2014, because it maintains a wider forecast band, while it does not produce overly large forecast intervals in high volatility regions, e.g. Oct 2014, Dec 2014 - Jan 2015. Therefore, the SR-SV model is less sensitive to the data values in the shorter time periods, and maintains a good trade-off between the information in recent observations and the information in the long-term memory. The SV, N-SV and LMSV models, compared to the SR-SV model, produce a smaller forecast volatility in low volatility regions and a higher volatility forecast in high volatility regions. The figure also shows that the SV and N-SV forecasts depend mainly on the return at the previous step, as the persistence parameters ϕ in the SV and N-SV models are larger than the persistence parameter of the SR-SV model. The SR-SV intervals are closer to the intervals made by the realized variance and hence seem to track the out-of-sample returns better than the SV, N-SV and LMSV models.

Table 12 shows the out-of-sample performances of the four models on the SPX data, with the Monte Carlo standard errors in brackets. Tables 15, 16, 17 and 18 in Appendix A.4 show the results for the other four datasets. Each table provides predictive scores separately in four panels, corresponding to the four realized measures BV, MedRV, RKV and RV, as discussed Section 4.2.1. In each panel, we count the number of times a particular model has lowest (best) predictive scores and list these numbers in the last column; the model with the highest count is preferred. We note that the PPS predictive score is independent of the realized measures

	Filtered volatility				Residual $\tilde{\epsilon}_t^y$			
	Mean	Std	Kurtosis	Skew	Std	Kurtosis	Skew	LB- $\hat{\epsilon}_t$
DAX								
SV	1.531	1.930	24.465	4.075	0.985	2.817	-0.215	0.978
N-SV	1.591	2.290	38.239	5.112	0.982	2.742	-0.213	0.978
LMSV	1.423	1.670	13.734	2.885	0.999	3.584	-0.163	0.887
SR-SV	1.325	1.559	26.276	4.182	0.991	2.819	-0.207	0.983
HSI								
SV	1.343	2.084	55.696	6.187	0.966	2.801	-0.040	0.162
N-SV	1.428	3.133	179.820	11.399	0.965	2.776	-0.040	0.226
LMSV	1.271	1.632	22.216	3.720	0.999	3.946	-0.028	0.326
SR-SV	1.101	1.651	50.909	5.821	0.978	2.768	-0.052	0.132
FCHI								
SV	1.416	1.563	13.561	2.851	0.982	2.724	-0.123	0.101
N-SV	1.483	1.867	22.140	3.705	0.981	2.690	-0.117	0.103
LMSV	1.287	1.451	11.815	2.645	1.000	3.548	-0.058	0.108
SR-SV	1.167	1.159	13.285	2.756	0.985	2.722	-0.136	0.105
SPX								
SV	1.648	2.712	25.696	4.395	0.994	2.769	-0.254	0.136
N-SV	1.729	3.139	33.443	5.010	0.995	2.737	-0.251	0.143
LMSV	1.592	2.810	25.516	4.381	0.999	3.623	-0.103	0.219
SR-SV	1.892	3.862	29.532	4.856	1.002	2.746	-0.252	0.149
TSX								
SV	1.543	2.516	27.582	4.641	0.971	2.705	-0.311	0.977
N-SV	1.590	2.846	35.343	5.256	0.971	2.683	-0.307	0.969
LMSV	1.395	2.124	20.325	3.893	0.999	3.353	-0.301	0.915
SR-SV	1.389	2.347	28.167	4.702	0.973	2.659	-0.310	0.961

Table 10: Applications: Model diagnostics of the filtered log volatility and residual $\tilde{\epsilon}_t^y$. The LB p-values denote the p-value from the Ljung-Box test with 10 lags.

of volatility, and that the PPS predictive score is not available for the LMSV model.

As shown in these tables, the SR-SV model consistently has the best out-of-sample performance in all the five index datasets. The superior predictive performance of the SR-SV model

	Forecast Volatility				Forecast Residual $\hat{\epsilon}_t^y$			
	Mean	Std	Kurtosis	Skew	Std	Kurtosis	Skew	LB- $\hat{\epsilon}_t$
DAX								
SV	1.069	0.580	2.992	0.711	0.997	3.964	-0.334	0.652
N-SV	1.072	0.588	3.464	0.893	0.992	3.937	-0.342	0.659
LMSV	1.083	0.616	3.467	0.879	1.001	3.942	-0.310	0.577
SR-SV	0.943	0.458	3.261	0.879	1.034	3.835	-0.328	0.597
HSI								
SV	0.655	0.380	14.099	2.823	0.982	4.353	0.036	0.390
N-SV	0.649	0.408	23.440	3.827	0.981	4.298	0.021	0.379
LMSV	0.740	0.386	9.633	2.065	0.928	4.465	0.057	0.283
SR-SV	0.491	0.215	15.963	3.102	1.091	4.135	-0.008	0.368
FCHI								
SV	1.087	0.620	3.796	0.989	0.963	4.590	-0.436	0.734
N-SV	1.089	0.646	4.629	1.249	0.965	4.415	-0.432	0.686
LMSV	1.144	0.633	5.126	1.400	0.971	4.656	-0.371	0.657
SR-SV	0.894	0.434	3.626	0.918	0.995	4.174	-0.375	0.609
SPX								
SV	0.675	0.438	9.938	2.135	0.983	3.970	-0.456	0.352
N-SV	0.679	0.453	12.583	2.503	0.978	3.970	-0.458	0.365
LMSV	0.763	0.422	4.993	1.291	0.920	4.075	-0.416	0.547
SR-SV	0.523	0.287	9.978	2.242	1.074	3.797	-0.406	0.450
TSX								
SV	0.551	0.314	3.231	0.976	0.960	3.859	-0.537	0.123
N-SV	0.551	0.304	3.412	1.035	0.952	3.811	-0.533	0.105
LMSV	0.541	0.272	3.156	0.798	0.983	4.060	-0.583	0.098
SR-SV	0.500	0.229	3.948	1.234	0.973	3.734	-0.502	0.077

Table 11: Applications: Summary statistics on the one-step-ahead out-of-sample forecast conditional variances $\hat{\sigma}_t^2$ and residual $\hat{\epsilon}_t$. The LB p-values denote the p-value from the Ljung-Box test with 10 lags.

is consistent with its in-sample performance discussed earlier and provides further evidence to support the conclusion that the SR-SV model does not overfit the five index datasets. We

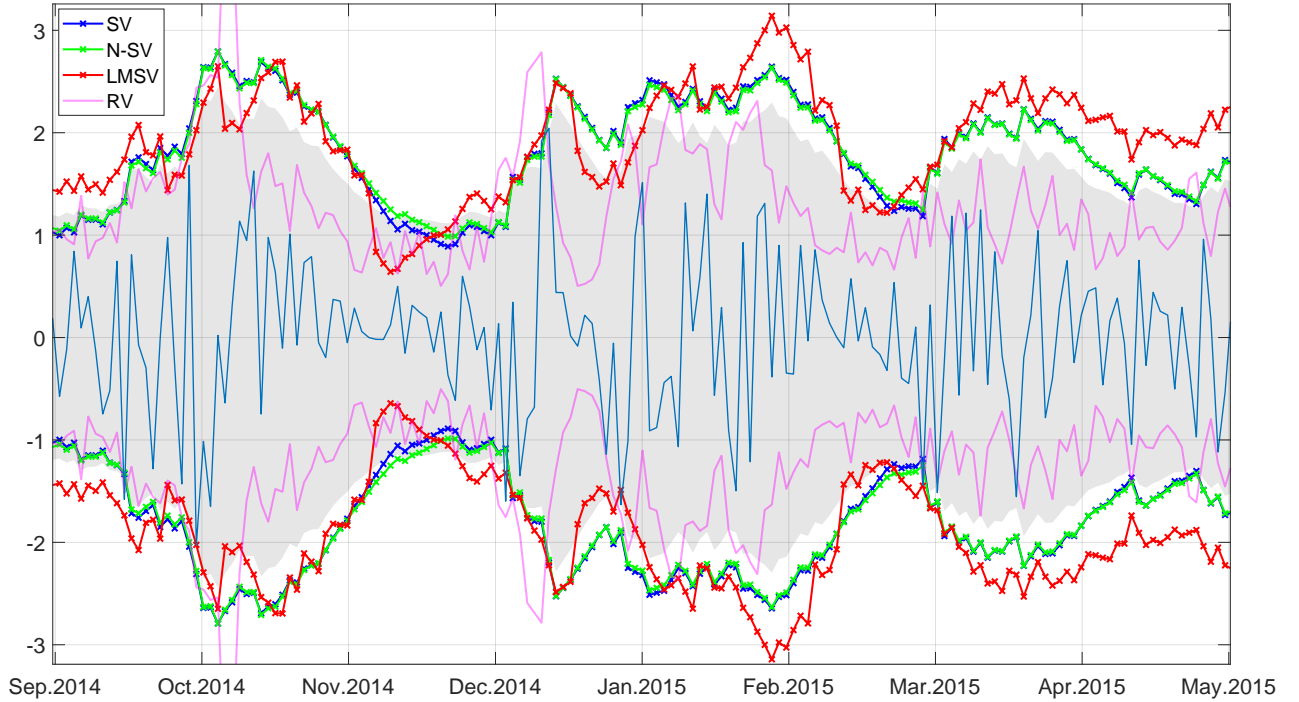


Figure 10: SPX: 99% One-step-ahead forecast intervals of the SR-SV, SV, N-SV and LMSV models, together with the 99% interval of index data estimated by the realized variance (RV) during Sep 2014 - May 2015. The shaded area is the 99% one-step-ahead forecast interval produced by the SR-SV model.

note that the forecast performances of the SV and N-SV models are mixed with no model consistently outperforming the other across the predictive scores and the datasets. The LMSV model consistently makes the least accurate forecasts in all cases .

5 Conclusions

This paper proposes a statistical recurrent stochastic volatility (SR-SV) model, by combining the statistical recurrent unit architecture from Machine Learning and the stochastic volatility model from Financial Econometrics. These two techniques are combined in a principled and non trivial way to form a new approach that is, as carefully illustrated through the extensive simulation and empirical studies, highly efficient for volatility modelling and forecasting. It is easy to carry Bayesian inference in the SR-SV model using standard Bayesian computation methods, such as the Density Tempered Sequential Monte Carlo method as used in this paper. The simulation and empirical studies suggest that the SR-SV model is able to capture various volatility effects overlooked by the SV benchmark models, and is able to produce highly accurate forecast volatilities.

Extending the SR-SV model by incorporating features such as the leverage effect is an interesting research question. Another interesting research question is extending the present SR-SV model to multivariate financial time series. We conjecture that the RNN architectures will be even more powerful in this case as they can naturally capture the interaction between the inputs. This research is in progress.

Measure		PPS	MSE ₁	MSE ₂	MAE ₁	MAE ₂	QLIKE	R ² LOG	Count
BV	SV	1.122 (0.001)	0.103 (0.001)	1.333 (0.002)	0.229 (0.001)	0.392 (0.002)	0.347 (0.001)	0.667 (0.002)	0
	N-SV	1.122 (0.000)	0.103 (0.001)	1.327 (0.002)	0.229 (0.001)	0.392 (0.002)	0.346 (0.001)	0.669 (0.003)	0
	LMSV		0.125	1.406	0.265	0.451	0.402	0.837	0
	SR-SV	1.113 (0.001)	0.091 (0.000)	1.321 (0.002)	0.209 (0.000)	0.354 (0.001)	0.330 (0.002)	0.572 (0.000)	7
MedRV	SV		0.114 (0.000)	0.830 (0.002)	0.256 (0.001)	0.428 (0.001)	0.323 (0.001)	0.862 (0.003)	0
	N-SV		0.114 (0.000)	0.826 (0.002)	0.257 (0.001)	0.428 (0.000)	0.323 (0.001)	0.866 (0.004)	0
	LMSV		0.140	0.901	0.294	0.488	0.385	1.064	0
	SR-SV		0.102 (0.000)	0.821 (0.002)	0.235 (0.000)	0.389 (0.000)	0.308 (0.001)	0.757 (0.001)	6
RKV	SV		0.114 (0.000)	0.834 (0.001)	0.256 (0.000)	0.419 (0.001)	0.363 (0.000)	0.915 (0.002)	0
	N-SV		0.114 (0.000)	0.829 (0.002)	0.256 (0.000)	0.420 (0.000)	0.361 (0.000)	0.918 (0.001)	0
	LMSV		0.137	0.904	0.290	0.476	0.405	1.100	0
	SR-SV		0.101 (0.000)	0.822 (0.001)	0.237 (0.000)	0.384 (0.000)	0.345 (0.000)	0.808 (0.001)	6
RV	SV		0.121 (0.000)	1.864 (0.002)	0.245 (0.001)	0.421 (0.002)	0.331 (0.000)	0.796 (0.002)	0
	N-SV		0.120 (0.000)	1.863 (0.002)	0.246 (0.001)	0.422 (0.001)	0.329 (0.001)	0.799 (0.003)	0
	LMSV		0.145	1.95	0.283	0.484	0.385	0.983	0
	SR-SV		0.108 (0.000)	1.861 (0.001)	0.224 (0.000)	0.382 (0.000)	0.316 (0.001)	0.692 (0.000)	6

Table 12: SPX data: Forecast performance of the SR-SV and benchmark models using different realized measures. In each panel, the bold numbers indicate the best predictive scores.

A Appendix

A.1 Bayesian inference and forecast for the LMSV model

Denote by $x = \{x_t = \log y_t^2, t = 1, \dots, T\}$ the series of log squared returns, the LMSV model in (5)-(6) can be transformed to a stationary process with respect to x_t as

$$(1 - B)^d \Phi(B) z_t = \Theta(B) \eta_t, \quad \eta_t \sim \mathcal{N}(0, \sigma_\eta^2), \quad t = 2, \dots, T, \quad (31)$$

$$x_t = c + z_t + \xi_t, \quad \xi_t \sim (0, \sigma_\xi^2) \quad t = 1, 2, \dots, T, \quad (32)$$

where $\xi_t = \log \epsilon_t^2 - \mathbb{E}[\log \epsilon_t^2]$ is i.i.d with mean zero and variance σ_ξ^2 , $c = \log(\kappa^2) + \mathbb{E}[\log \epsilon_t^2]$. The process x_t is the sum of the long-memory ARFIMA(p, d, q) process z_t and a non-Gaussian noise, with $\mathbb{E}[x_t] = c$ and the auto-covariance function (ACVF)

$$\gamma_x(h) = \text{Cov}(x_t, x_{t+h}) = \gamma(h) + \sigma_\xi^2 \mathbb{1}_{h=0}, \quad (33)$$

where h is the lag number, $\gamma(h)$ is the ACVF of the z_t process and $\mathbb{1}_{h=0}$ is an indicator function which equals to 1 if $h=0$ and 0 otherwise. Breidt et al. (1998) estimate the LMSV model by maximizing the Whittle log-likelihood (Whittle, 1953), defined as

$$\ell_W(\beta_x) = 2\pi T^{-1} \sum_{k=1}^{[T/2]} \left\{ \log f_{\beta_x}(\omega_k) + \frac{J(\omega_k)}{f_{\beta_x}(\omega_k)} \right\}, \quad (34)$$

where $[\cdot]$ denotes the integer part, $\beta_x = (d, \phi_1, \dots, \phi_p, \theta_1, \dots, \theta_q, \sigma_\eta^2, \sigma_\xi^2, c)$ is the vector of model parameters, $\omega_k = 2\pi k T^{-1}$ is the k th Fourier frequency, $J(\omega_k)$ is the k th normalized periodogram ordinate

$$J(\omega_k) = \frac{1}{2\pi T} \left(\sum_{t=1}^T x_t \cos \omega_k t \right)^2 + \frac{1}{2\pi T} \left(\sum_{t=1}^T x_t \sin \omega_k t \right)^2, \quad (35)$$

and $f_{\beta_x}(\omega_k)$ is the spectral density of the LMSV model in (31)-(32)

$$f_{\beta_x}(\omega_k) = \frac{\sigma_\eta^2 |\Theta(e^{-i\omega_k})|^2}{2\pi |1 - e^{-i\omega_k}|^{2d} |\Phi(e^{-i\omega_k})|^2} + \frac{\sigma_\xi^2}{2\pi}. \quad (36)$$

The Whittle likelihood is an approximation of the time-domain likelihood and is exact if the data are i.i.d. Gaussian.

Let $\pi_W(\beta_x) \propto L_W(\beta_x) p(\beta_x)$ be the posterior density based on the Whittle likelihood $L_W(\beta_x) = \exp(\ell_W(\beta_x))$, given the log of squared return series $x = \{x_t, t=1, \dots, T\}$. To sample from $\pi_W(\beta_x)$, we use an adaptive random walk MCMC method summarized in Algorithm 2, with the covariance matrix in the random walk proposal adaptively scaled to target an overall acceptance probability of 25% Garthwaite et al. (2010). We note that the vector of parameters β_x in Algorithm 2 does not include the constant c in (32), which is simply estimated by the sample mean, i.e., $c = \frac{1}{T} \sum_{t=1}^T x_t$ (Harvey, 2007).

Given the samples of model parameters from the posterior density $\pi_W(\beta_x)$, Harvey (2007) suggests a convenient way to obtain the estimated values of conditional variance σ_t^2 for the LMSV model as follows. Suppose that z_t is a stationary process and denote by Σ_z and Σ_ξ the covariance matrices of z_t and ξ_t , respectively, then the covariance matrix Σ of the log squared returns series x is $\Sigma = \Sigma_z + \Sigma_\xi$. The minimum mean square linear estimator of the log volatility $\tilde{z} = \{\tilde{z}_t, t=1, \dots, T\}$ is calculated as

$$\tilde{z} = (\mathbf{I}_T - \sigma_\xi^2 \Sigma^{-1}) x' + \sigma_\xi^2 \Sigma^{-1} \mathbf{1}, \quad (37)$$

where \mathbf{I}_T is the identity matrix of size T , $\mathbf{1}$ is a $T \times 1$ column vector of ones. As ξ_t are i.i.d and serially uncorrelated, the covariance matrix Σ_ξ is $\Sigma_\xi = \sigma_\xi^2 \mathbf{I}_T$. We note that for a general ARFIMA(p, d, q) process, there is no closed form for the ACVF $\gamma(h)$, and hence covariance matrix Σ_z , so approximations of Σ_z are needed, e.g. see Sowell (1992); Doornik and Ooms

Algorithm 2 Markov Chain Monte Carlo with random walk proposal

Sample $\beta_x \sim p(\beta_x)$

For each MCMC iteration:

1. Sample β'_x from the proposal density $q(\beta'_x|\beta_x)$.
2. Compute the Whittle likelihood $L_W(\beta'_x) = \exp(\mathcal{L}_w(\beta'_x))$ with $\mathcal{L}_w(\cdot)$ defined in (34).
3. Accept the proposal β'_x with the probability

$$\min \left\{ 1, \frac{L_W(\beta'_x) p(\beta'_x) q(\beta_x|\beta'_x)}{L_W(\beta_x) p(\beta_x) q(\beta'_x|\beta_x)} \right\}.$$

(2003). However, Hosking (1981) suggests exact ACVF for some simple cases of (p, d, q) such as ARFIMA(0, d , 0), ARFIMA(1, d , 0) and ARFIMA(0, d , 1).

Given the estimates of z_t in (37), the conditional variance σ_t^2 is computed as

$$\tilde{\sigma}_t^2 = \tilde{\kappa}^2 \exp(\tilde{z}_t),$$

where the scale factor $\tilde{\kappa}^2$ is estimated as

$$\tilde{\kappa}^2 = \frac{1}{T} \sum_{t=1}^T \tilde{y}_t, \quad (38)$$

with $\tilde{y}_t = y_t \exp(-\tilde{z}_t/2)$ the heteroscedasticity corrected observations.

Denote by R the $1 \times T$ the vector of covariance between x_{T+1} and x , e.g. $R = [\gamma_x(1), \dots, \gamma_x(T)]$, the one-step-ahead forecast value of the log squared return is calculated as (Harvey, 2007)

$$\hat{x}_{T+1} = c + R\Sigma^{-1}(x - c\mathbf{1}_T)$$

The one-step-ahead forecast of the conditional variance is $\hat{\sigma}_{T+1} = \tilde{\kappa}^2 \exp(\hat{x}_{T+1} - c)$.

Table 13 shows the estimation results of the LMSV model using a ARFIMA(1, d , 0) process to model the log volatility z_t , with the vector of parameters $\beta_x = [d, \phi_1, \sigma_\eta^2, \sigma_\xi^2]$. We also report the estimation of the scale factor κ in (6) and the constant c in (32). For the parameters ϕ_1 and σ_η^2 , we choose the priors to be similar to those of the SV model as shown in Table 2. We use the same inverse-Gamma prior, as that of σ_η^2 , for the parameter σ_ξ^2 . For the fractional integration parameter d , we set the prior $2d \sim \text{Beta}(20, 5)$. We run $N_{\text{MCMC}} = 100000$ MCMC iterations of Algorithm 2 and then discard the first 10,000 iterations as burn-ins.

	d	ϕ	σ_η^2	σ_ξ^2	κ	c
DAX	0.442 (0.026)	0.708 (0.082)	0.054 (0.024)	4.933 (0.170)	1.974	-1.616
HSI	0.431 (0.030)	0.747 (0.069)	0.052 (0.021)	5.469 (0.183)	2.047	-1.526
FCHI	0.434 (0.029)	0.716 (0.083)	0.062 (0.029)	5.241 (0.182)	1.984	-1.562
SPX	0.428 (0.035)	0.809 (0.060)	0.040 (0.016)	5.488 (0.177)	2.017	-1.650
TSX	0.445 (0.026)	0.714 (0.084)	0.047 (0.021)	4.964 (0.160)	1.918	-1.493

Table 13: Applications: Posterior means of the parameters of the LMSV model with the posterior standard deviations in brackets. We also report the estimation of the scale factor κ and the constant c .

A.2 The SR-SV model

The SR-SV model in Section 2.3 is fully written as

$$\begin{aligned}
r_t &= \Psi(w_h h_{t-1} + b_r) \\
\varphi_t &= \Psi(w_r r_t + w_\eta \eta_{t-1} + w_z z_{t-1} + b_\varphi) \\
h_t &= \alpha h_{t-1} + (1 - \alpha) \varphi_t \\
\eta_t &= \beta_0 + \beta_1 h_t + \epsilon_t^\eta, \quad \epsilon_t^\eta \stackrel{iid}{\sim} \mathcal{N}(0, \sigma^2), \quad t = 1, 2, \dots, T \\
z_t &= \eta_t + \phi z_{t-1}, \quad t = 1, \dots, T, \\
y_t &= e^{\frac{1}{2} z_t} \epsilon_t^y, \quad \epsilon_t^y \stackrel{iid}{\sim} \mathcal{N}(0, 1), \quad t = 1, 2, \dots, T,
\end{aligned}$$

where $\Psi(\cdot)$ is the ReLU activation function, $\Psi(x) = \max(0, x)$. The model parameter vector is $\theta = (\beta_0, \beta_1, \phi, \sigma^2, \alpha, w_h, b_r, w_r, b_\varphi, w_\eta, w_z)$.

A.3 Particle filter and implementation details of the DT-SMC sampler

Algorithm 3 describes the particle filter for the SR-SV model where $\mathbf{Z}_t = (Z_t^1, \dots, Z_t^N)$ denotes the vector of particles at time t . The set of standard normal random numbers U includes two sources of randomness: the set of random numbers $\{U_{t,k}^P, t=1, \dots, T; k=1, \dots, N\}$ used to propose new particles in each time step, and the set of random numbers $\{U_{t,k}^R, t=1, \dots, T-1; k=1, \dots, N\}$ used in the resampling step. For the resampling step, we use multinomial resampling, with sorting, to obtain the vector ancestor indexes $\{A_{t-1}^k, k=1, \dots, N\}$ used to propose particles at time t . The sorting step helps eliminate the discontinuity issues of the selected particles in the ordinary multinomial resampling scheme (Gerber and Chopin, 2014). This sorted resampling scheme allows the selected particles to still be close after being resampled and hence helps to reduce the variability of the likelihood ratio estimator $\hat{p}(y_{1:T}|\theta', u')/\hat{p}(y_{1:T}|\theta, u)$ shown in the Algorithm 1 (Deligiannidis et al., 2018).

The multinomial resampling scheme in step 2a and 2b generates the ancestor index $A_{t-1}^k, k=1, \dots, N$, from the multinomial distribution denoted as $\mathcal{F}(\cdot|\mathbf{p}, \mathbf{u})$ with \mathbf{p} the vector of parameters

Variable	Description	Value
K	Number of annealing levels	10000
M	Number of particles	10000
N	Number of particles in the particle filter	200
ρ	Correlation factor in the CPM algorithm	0.999
c	Constant of the ESS threshold	0.800
N_{CPM}	Number of CPM moves	20

Table 14: Implementation settings of the DT-SMC sampler.

of the multinomial distribution and \mathbf{u} the uniform random numbers used within a multinomial random number generator. We use the standard normal cumulative distribution function $\Phi(\cdot)$ in the resampling step to transform the normal random numbers $U_{t-1,k}^R$ to the uniform random numbers, denoted as $\bar{U}_{t-1,k}^R$.

A.4 Additional results

This section provides the additional tables and figures discussed in Section 4.2.

Algorithm 3 Particle filter for the SR-SV model

Input: $T, N, y_{1:T}, \theta, U = (U_{1,1}^P, \dots, U_{T,N}^P, U_{1,1}^R, \dots, U_{T-1,N}^R)$

1. At time $t=1$,

(a) for $k=1, \dots, N$, initialize the particles (H_1^k, η_1^k, Z_1^k) , e.g., $H_1^k=0$, as the SRU unit initially has no memory, and

$$\begin{aligned}\eta_1^k &= \beta_0 + \sigma U_{1,k}^P \\ Z_1^k &= \eta_1^k\end{aligned}$$

(b) compute and normalize the weights

$$\begin{aligned}w_1(Z_1^k) &= \frac{\mu_\theta(Z_1^k) g_\theta(y_1 | Z_1^k)}{q_\theta(Z_1^k | y_1)} = g_\theta(y_1 | Z_1^k) \\ W_1^k &= \frac{w_1(Z_1^k)}{\sum_{m=1}^N w_1(Z_1^m)}\end{aligned}$$

(c) compute the estimated likelihood $\hat{p}(y_1 | \theta)$ as

$$\hat{p}(y_1 | \theta, U) = \frac{1}{N} \sum_{k=1}^N w_1(Z_1^k).$$

2. At times $t=2, \dots, T$,

(a) sort the particle vector \mathbf{Z}_{t-1} in ascending order to obtain the vector of sorted particles $\bar{\mathbf{Z}}_{t-1} = (\bar{Z}_{t-1}^1, \dots, \bar{Z}_{t-1}^N)$. The sorted index vector associated with $\bar{\mathbf{Z}}_{t-1}$ is denoted as $\mathbf{I}_{t-1} = (I_{t-1}^1, \dots, I_{t-1}^N)$. In this setting, we have the relation $\bar{Z}_{t-1}^k = Z_{t-1}^{I_{t-1}^k}$ with $k=1, \dots, N$. Use the sorted index vector \mathbf{I}_{t-1} to define the vector of sorted weights $(\bar{W}_{t-1}^1, \dots, \bar{W}_{t-1}^N)$ such that

$$\bar{W}_{t-1}^k = W_{t-1}^{I_{t-1}^k}$$

(b) sample $A_{t-1}^k \sim \mathcal{F}(\cdot | \bar{W}_{t-1}^k, \bar{U}_{t-1,k}^R)$ where $\bar{U}_{t-1,k}^R = \Phi(U_{t-1,k}^R)$ for $k=1, \dots, N$.

(c) for $k=1,\dots,N$, generate particles Z_t^k by

$$\begin{aligned} x_{t-1} &= [\eta_{t-1}^{A_{t-1}^k}, Z_{t-1}^{A_{t-1}^k}] \\ H_t^k &= \text{SRU}(x_{t-1}, H_{t-1}^{A_{t-1}^k}) \\ \eta_t^k &= \beta_0 + \beta_1 H_t^k + \sigma U_{t,k}^P \\ Z_t^k &= \eta_t^k + \phi Z_{t-1}^{A_{t-1}^k} \end{aligned}$$

and set $Z_{1:t}^k = (Z_{1:t-1}^{A_{t-1}^k}, Z_t^k)$.

(d) compute and normalize the weights

$$\begin{aligned} w_t(Z_{1:t}^k) &= \frac{f_\theta(Z_t^k | Z_{t-1}^{A_{t-1}^k}) g_\theta(y_t | Z_t^k)}{q_\theta(Z_t^k | y_t, Z_{t-1}^{A_{t-1}^k})} = g_\theta(y_1 | Z_1^k) \\ W_t^k &= \frac{w_t(Z_{1:t}^k)}{\sum_{m=1}^N w_t(Z_{1:t}^m)} \end{aligned}$$

(e) compute the estimated likelihood $\hat{p}(y_t | y_{1:t-1}, \theta)$ as

$$\hat{p}(y_t | y_{1:t-1}, \theta, U) = \frac{1}{N} \sum_{k=1}^N w_t(Z_{1:t}^k).$$

Output: Estimate of the likelihood

$$\hat{p}(y_{1:T} | \theta, U) = \hat{p}(y_1 | \theta, U) \prod_{t=2}^T \hat{p}(y_t | y_{1:t-1}, \theta, U).$$

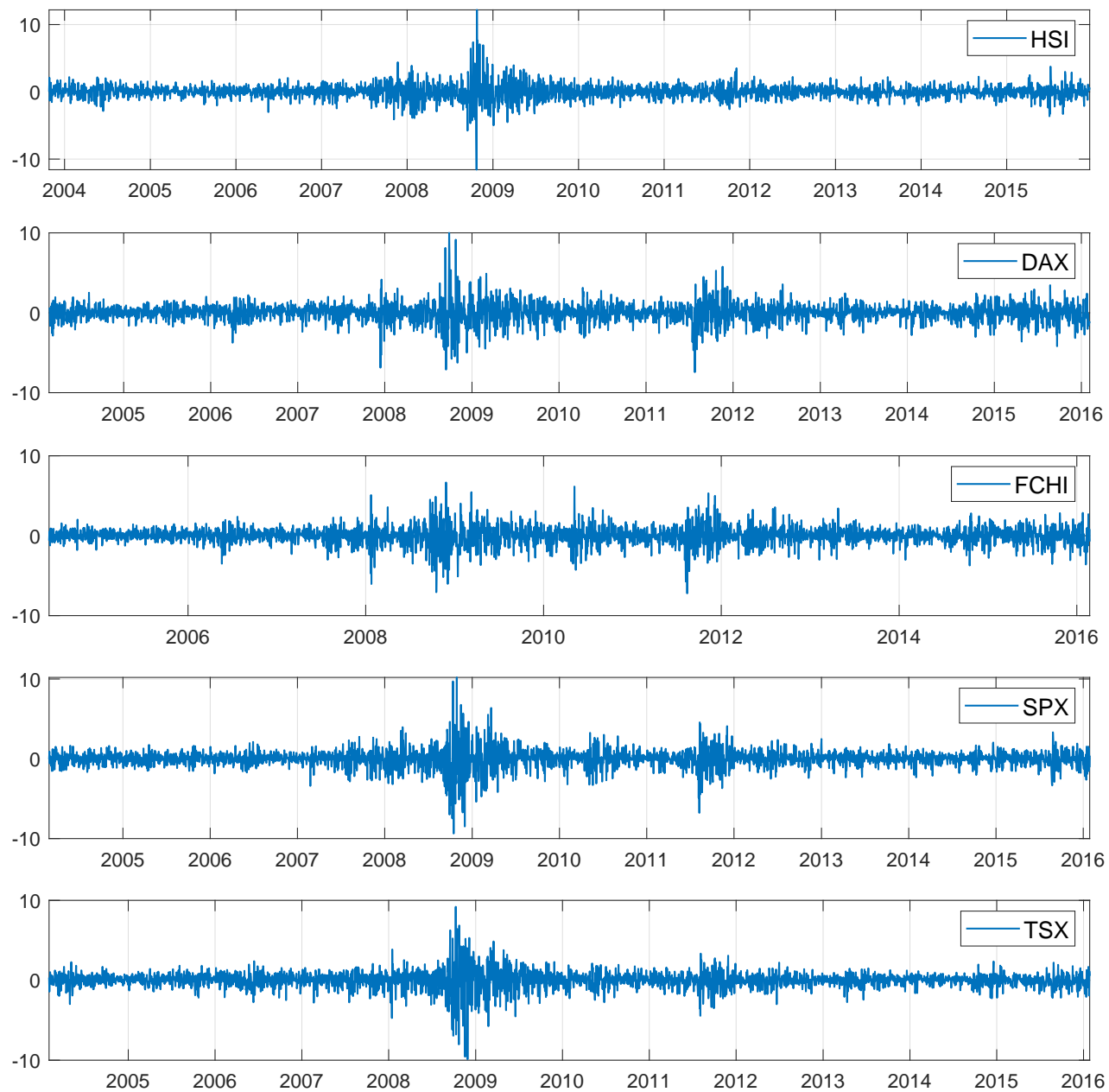


Figure 11: Applications: Time series plots for the HSI, DAX, FCHI, SPX and TSX datasets.

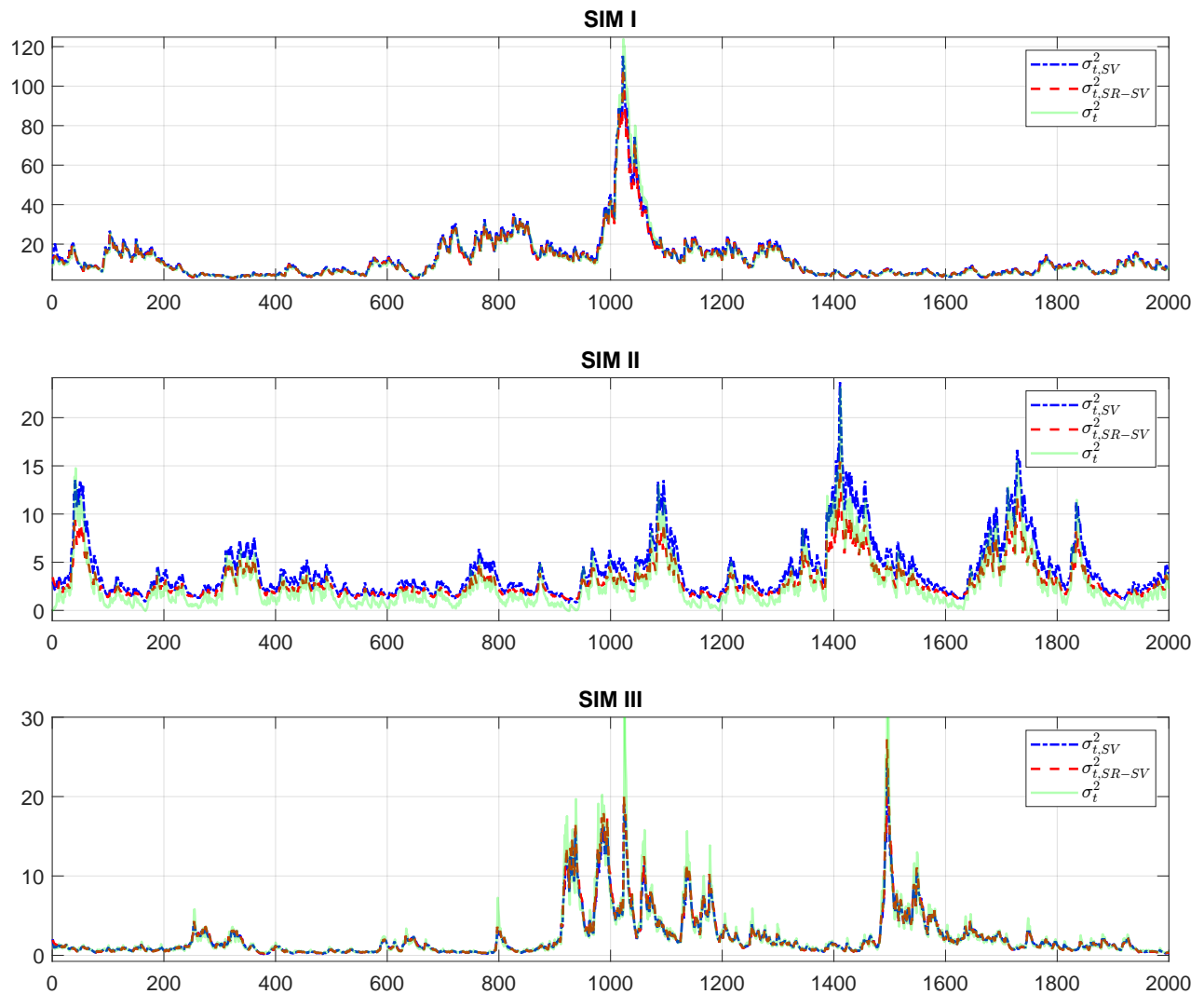


Figure 12: Simulation: Filtered volatility of the SV and SR-SV models, together with the true volatility, on three simulation datasets. (This is better viewed in colour).

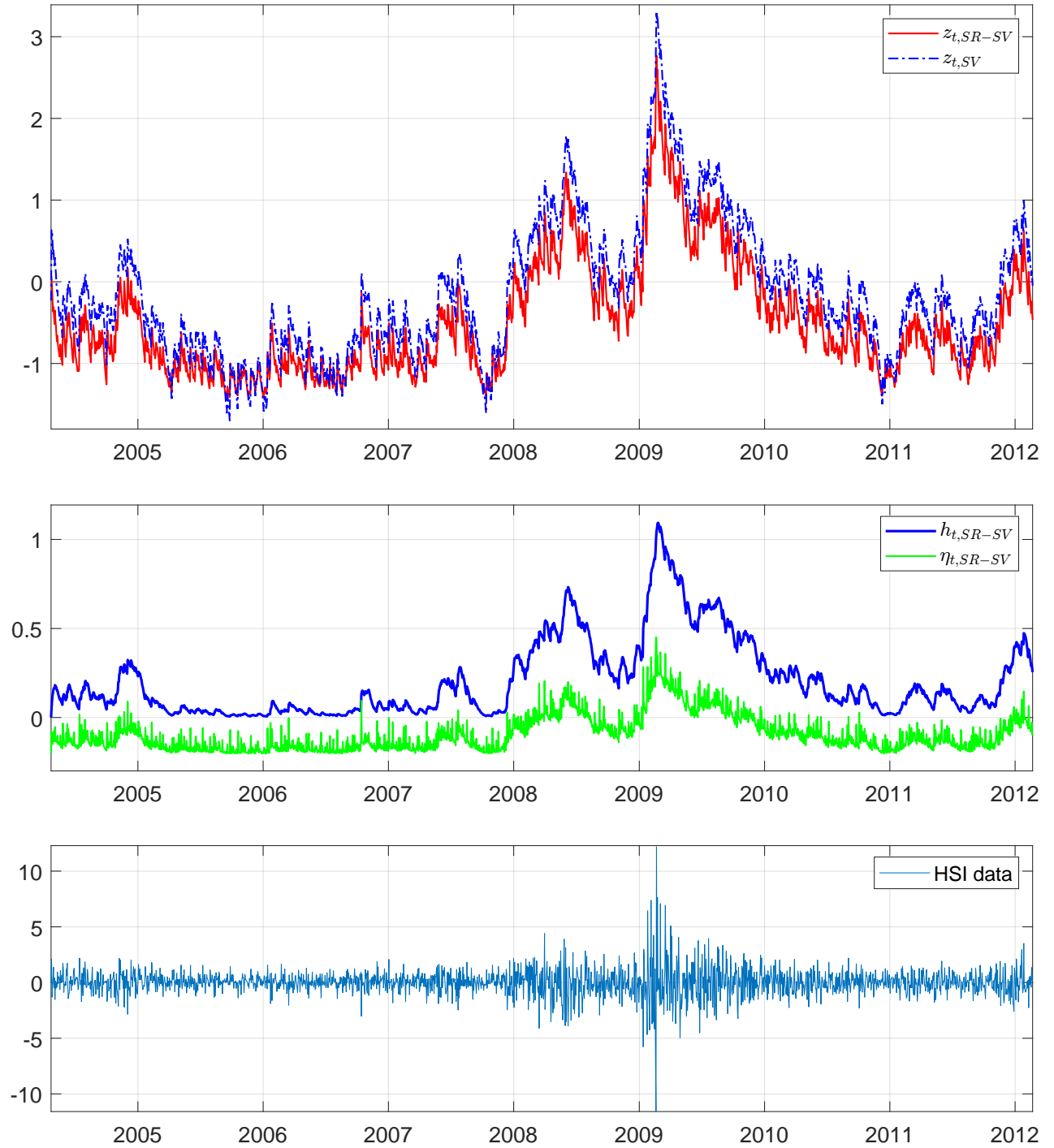


Figure 13: HSI: (*Top*) The filtered log conditional variance of the SR-SV and SV models. (*Middle*) The filtered values of η_t and h_t of the SR-SV model. (*Bottom*) The in-sample data. (This is better viewed in colour).

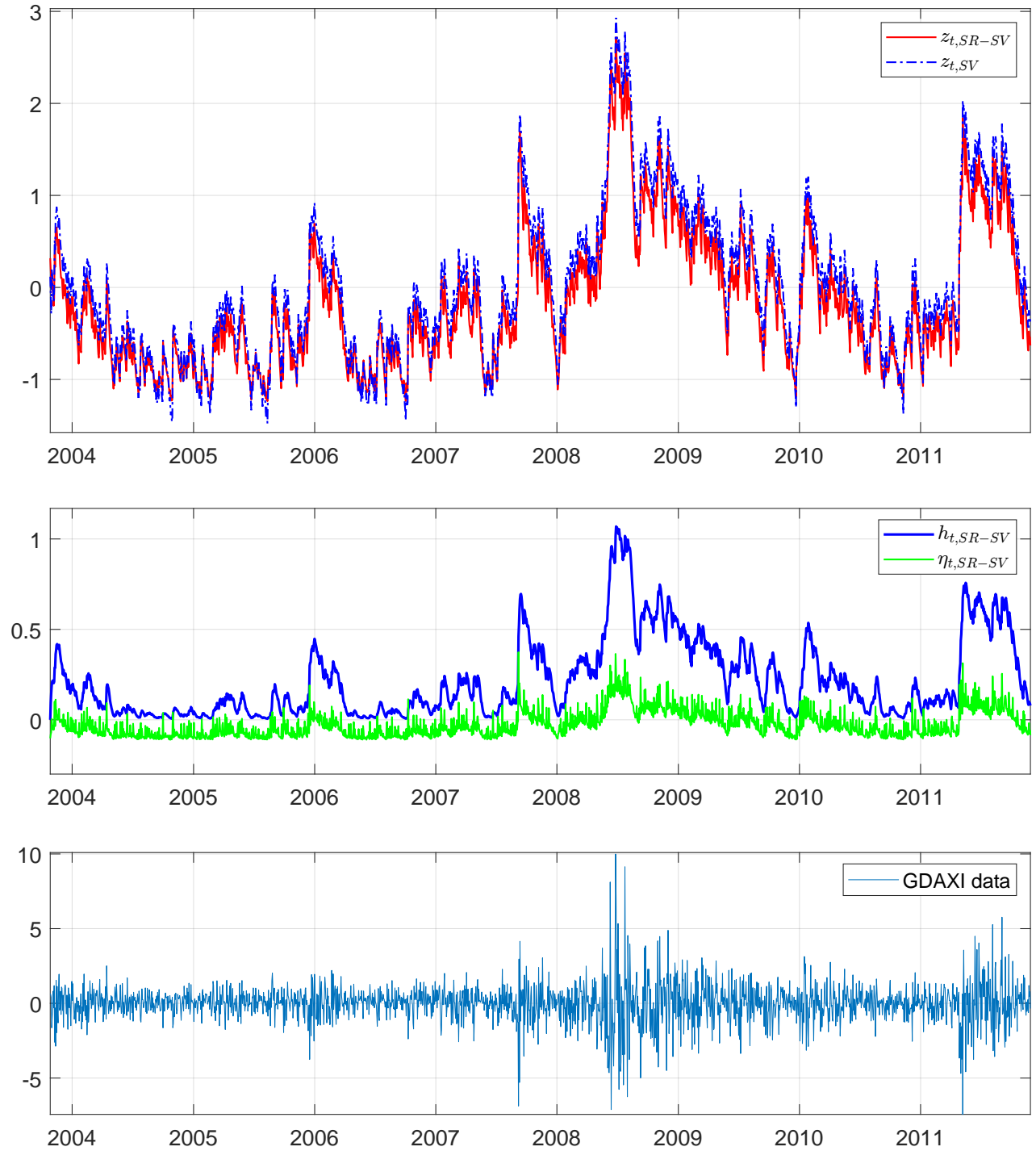


Figure 14: DAX: (*Top*) The filtered log conditional variance of the SR-SV and SV models. (*Middle*) The filtered values of η_t and h_t of the SR-SV model. (*Bottom*) The in-sample data. (This is better viewed in colour).

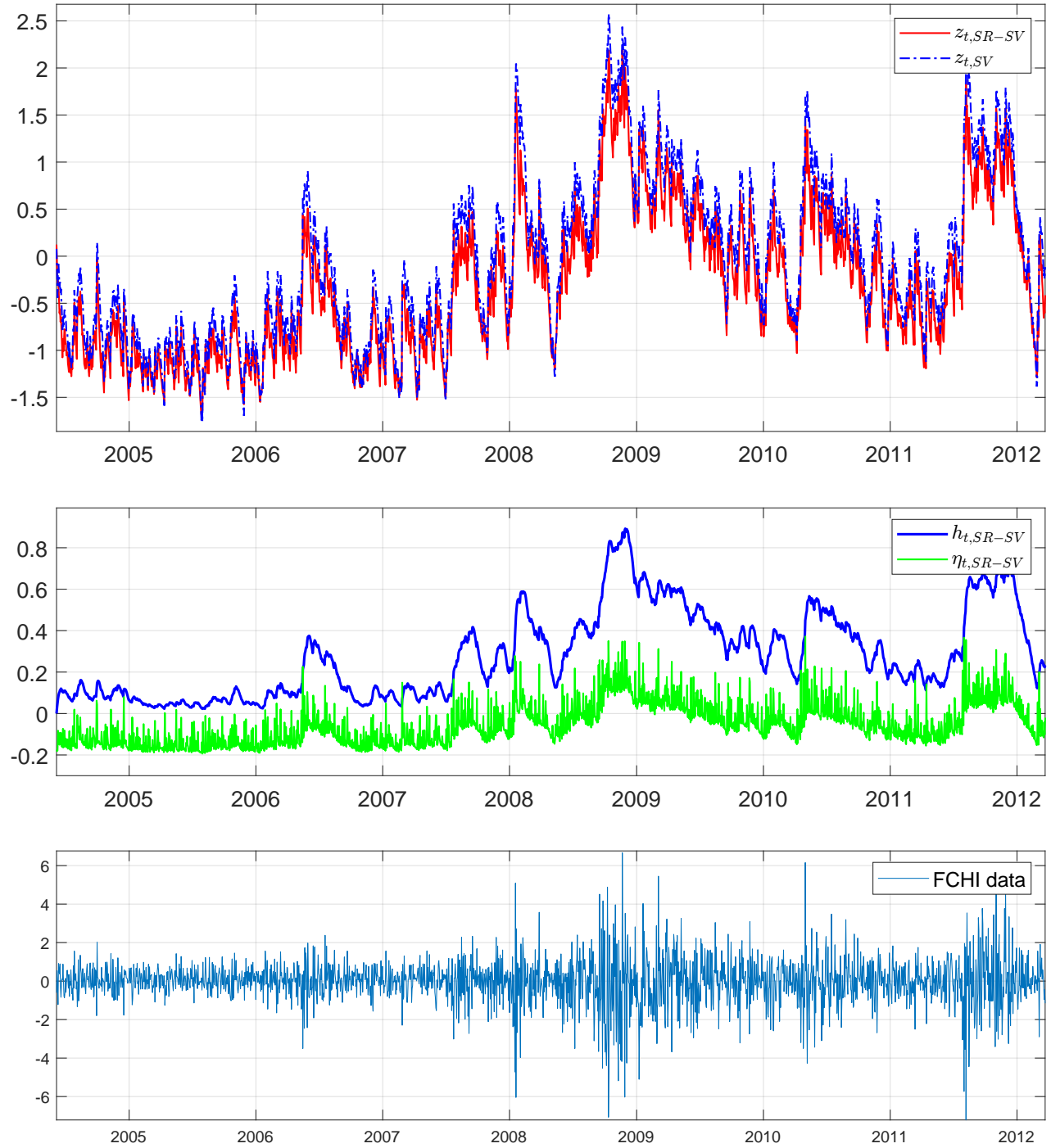


Figure 15: FCHI: (*Top*) The filtered log conditional variance of the SR-SV and SV models. (*Middle*) The filtered values of η_t and h_t of the SR-SV model. (*Bottom*) The in-sample data. (This is better viewed in colour).

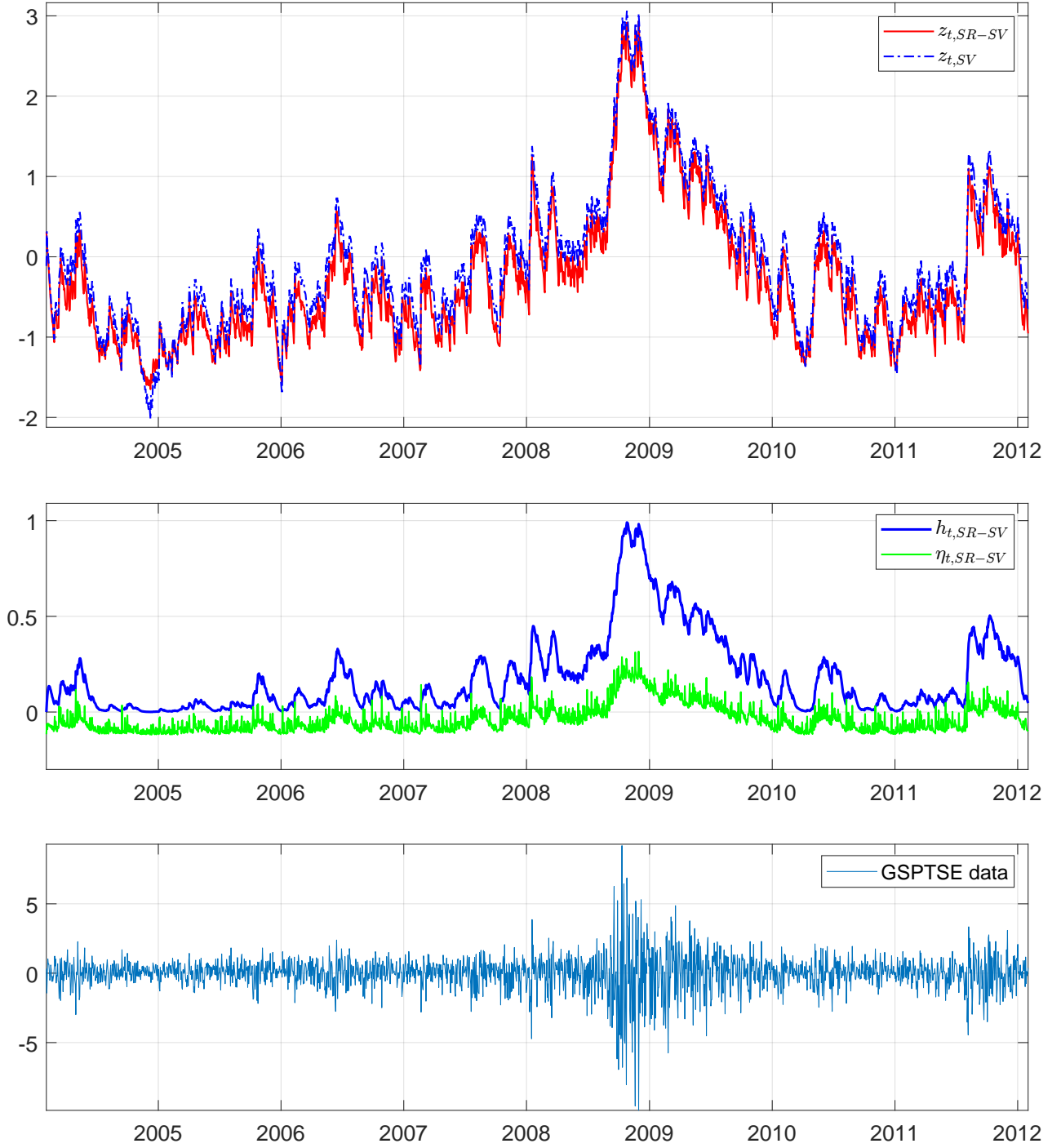


Figure 16: TSX: (*Top*) The filtered log conditional variance of the SR-SV and SV models. (*Middle*) The filtered values of η_t and h_t of the SR-SV model. (*Bottom*) The in-sample data. (This is better viewed in colour).

Measure		PPS	MSE ₁	MSE ₂	MAE ₁	MAE ₂	QLIKE	R ² LOG	Count
BV	SV	1.368 (0.000)	0.099 (0.000)	0.763 (0.001)	0.234 (0.000)	0.485 (0.000)	0.853 (0.000)	0.423 (0.000)	0
	N-SV	1.368 (0.000)	0.099 (0.001)	0.769 (0.003)	0.234 (0.001)	0.487 (0.002)	0.850 (0.001)	0.422 (0.002)	0
	LMSV		0.108	0.805	0.245	0.501	0.862	0.435	0
	SR-SV	1.365 (0.000)	0.09 (0.000)	0.745 (0.001)	0.220 (0.000)	0.452 (0.001)	0.847 (0.000)	0.386 (0.001)	7
MedRV	SV		0.094 (0.000)	0.582 (0.002)	0.237 (0.000)	0.486 (0.000)	0.810 (0.000)	0.443 (0.001)	0
	N-SV		0.094 (0.001)	0.585 (0.004)	0.238 (0.001)	0.489 (0.002)	0.810 (0.001)	0.447 (0.002)	0
	LMSV		0.099	0.612	0.245	0.504	0.825	0.467	0
	SR-SV		0.088 (0.000)	0.580 (0.001)	0.227 (0.000)	0.462 (0.001)	0.807 (0.000)	0.417 (0.001)	6
RKV	SV		0.126 (0.000)	0.994 (0.001)	0.268 (0.000)	0.558 (0.000)	0.858 (0.000)	0.581 (0.001)	0
	N-SV		0.126 (0.001)	1.001 (0.003)	0.269 (0.001)	0.559 (0.001)	0.854 (0.001)	0.581 (0.002)	0
	LMSV		0.135	1.023	0.279	0.578	0.878	0.603	0
	SR-SV		0.116 (0.000)	0.974 (0.001)	0.254 (0.000)	0.516 (0.000)	0.851 (0.000)	0.538 (0.001)	6
RV	SV		0.107 (0.000)	0.909 (0.001)	0.239 (0.000)	0.501 (0.000)	0.859 (0.000)	0.442 (0.001)	0
	N-SV		0.108 (0.001)	0.915 (0.003)	0.239 (0.001)	0.503 (0.002)	0.855 (0.001)	0.441 (0.002)	0
	LMSV		0.115	0.936	0.250	0.527	0.875	0.464	0
	SR-SV		0.098 (0.000)	0.889 (0.001)	0.223 (0.000)	0.462 (0.001)	0.851 (0.000)	0.400 (0.001)	6

Table 15: DAX data: Forecast performance of the SR-SV and benchmark models using different realized measures. In each panel, the bold numbers indicate the best predictive scores.

Measure		PPS	MSE ₁	MSE ₂	MAE ₁	MAE ₂	QLIKE	R ² LOG	Count
BV	SV	1.131 (0.000)	0.069 (0.000)	0.497 (0.001)	0.186 (0.000)	0.319 (0.001)	0.359 (0.001)	0.390 (0.001)	1
	N-SV	1.130 (0.000)	0.067 (0.000)	0.499 (0.001)	0.182 (0.000)	0.313 (0.001)	0.357 (0.001)	0.376 (0.002)	0
	LMSV		0.076	0.516	0.205	0.343	0.370	0.423	0
	SR-SV	1.127 (0.000)	0.060 (0.00)	0.504 (0.002)	0.152 (0.000)	0.261 (0.000)	0.355 (0.000)	0.294 (0.001)	5
MedRV	SV		0.066 (0.000)	0.371 (0.001)	0.191 (0.000)	0.317 (0.001)	0.347 (0.000)	0.435 (0.001)	0
	N-SV		0.065 (0.001)	0.370 (0.000)	0.188 (0.001)	0.312 (0.000)	0.344 (0.001)	0.423 (0.002)	1
	LMSV		0.073	0.396	0.207	0.335	0.356	0.469	0
	SR-SV		0.059 (0.000)	0.389 (0.001)	0.164 (0.000)	0.272 (0.001)	0.341 (0.000)	0.338 (0.001)	5
RKV	SV		0.100 (0.000)	0.740 (0.001)	0.230 (0.000)	0.385 (0.001)	0.366 (0.001)	0.665 (0.001)	1
	N-SV		0.098 (0.000)	0.741 (0.002)	0.226 (0.001)	0.380 (0.001)	0.364 (0.000)	0.648 (0.002)	0
	LMSV		0.112	0.764	0.246	0.405	0.380	0.744	0
	SR-SV		0.087 (0.000)	0.748 (0.002)	0.194 (0.000)	0.323 (0.001)	0.360 (0.000)	0.519 (0.001)	5
RV	SV		0.069 (0.000)	0.522 (0.001)	0.186 (0.000)	0.318 (0.001)	0.367 (0.001)	0.390 (0.001)	1
	N-SV		0.068 (0.000)	0.524 (0.001)	0.181 (0.000)	0.311 (0.001)	0.365 (0.001)	0.374 (0.002)	0
	LMSV		0.077	0.552	0.204	0.353	0.386	0.419	0
	SR-SV		0.060 (0.000)	0.530 (0.002)	0.150 (0.000)	0.258 (0.000)	0.361 (0.001)	0.291 (0.001)	5

Table 16: HSI data: Forecast performance of the SR-SV and benchmark models using different realized measures. In each panel, the bold numbers indicate the best predictive scores.

Measure		PPS	MSE ₁	MSE ₂	MAE ₁	MAE ₂	QLIKE	R ² LOG	Count
BV	SV	1.384 (0.000)	0.108 (0.000)	1.076 (0.001)	0.235 (0.000)	0.504 (0.001)	0.863 (0.000)	0.426 (0.001)	0
	N-SV	1.383 (0.000)	0.108 (0.000)	1.086 (0.002)	0.234 (0.000)	0.507 (0.001)	0.860 (0.000)	0.420 (0.001)	0
	LMSV		0.118	1.104	0.246	0.527	0.872	0.469	0
	SR-SV	1.381 (0.000)	0.095 (0.00)	1.057 (0.001)	0.210 (0.000)	0.448 (0.001)	0.856 (0.000)	0.354 (0.001)	7
MedRV	SV		0.100 (0.000)	0.670 (0.001)	0.238 (0.000)	0.500 (0.001)	0.833 (0.001)	0.543 (0.002)	0
	N-SV		0.100 (0.000)	0.672 (0.002)	0.237 (0.001)	0.501 (0.000)	0.832 (0.000)	0.538 (0.001)	0
	LMSV		0.112	0.695	0.247	0.513	0.849	0.582	0
	SR-SV		0.090 (0.000)	0.665 (0.001)	0.216 (0.000)	0.452 (0.000)	0.828 (0.000)	0.472 (0.001)	6
RKV	SV		0.158 (0.000)	1.271 (0.001)	0.301 (0.000)	0.624 (0.001)	0.901 (0.000)	0.750 (0.002)	0
	N-SV		0.159 (0.000)	1.285 (0.002)	0.301 (0.000)	0.628 (0.000)	0.896 (0.000)	0.745 (0.001)	0
	LMSV		0.168	1.332	0.315	0.656	0.908	0.815	0
	SR-SV		0.139 (0.000)	1.229 (0.001)	0.275 (0.000)	0.562 (0.000)	0.890 (0.000)	0.645 (0.001)	6
RV	SV		0.103 (0.000)	0.908 (0.001)	0.232 (0.000)	0.495 (0.000)	0.877 (0.000)	0.411 (0.001)	0
	N-SV		0.103 (0.000)	0.920 (0.002)	0.232 (0.000)	0.498 (0.001)	0.873 (0.000)	0.404 (0.001)	0
	LMSV		0.113	0.945	0.245	0.521	0.884	0.449	0
	SR-SV		0.090 (0.000)	0.880 (0.001)	0.209 (0.000)	0.440 (0.000)	0.869 (0.000)	0.340 (0.001)	6

Table 17: FCHI data: Forecast performance of the SR-SV and benchmark models using different realized measures. In each panel, the bold numbers indicate the best predictive scores and the model with highest count of best predictive scores is preferred.

Measure		PPS	MSE ₁	MSE ₂	MAE ₁	MAE ₂	QLIKE	R ² LOG	Count
BV	SV	1.004 (0.001)	0.074 (0.000)	0.904 (0.002)	0.192 (0.001)	0.295 (0.001)	0.106 (0.001)	0.542 (0.003)	0
	N-SV	1.003 (0.000)	0.074 (0.000)	0.902 (0.002)	0.192 (0.001)	0.294 (0.001)	0.105 (0.001)	0.543 (0.002)	1
	LMSV		0.091	0.965	0.217	0.331	0.197	0.676	0
	SR-SV	1.001 (0.000)	0.069 (0.00)	0.900 (0.001)	0.181 (0.000)	0.273 (0.001)	0.107 (0.001)	0.517 (0.001)	6
MedRV	SV		0.074 (0.000)	0.289 (0.001)	0.210 (0.001)	0.310 (0.001)	0.098 (0.001)	1.052 (0.002)	0
	N-SV		0.073 (0.000)	0.291 (0.002)	0.210 (0.001)	0.309 (0.000)	0.098 (0.001)	1.044 (0.001)	0
	LMSV		0.096	0.360	0.239	0.353	0.209	0.839	0
	SR-SV		0.069 (0.000)	0.287 (0.001)	0.201 (0.000)	0.291 (0.000)	0.098 (0.001)	0.985 (0.001)	5
RKV	SV		0.096 (0.000)	0.349 (0.001)	0.246 (0.000)	0.357 (0.001)	0.134 (0.000)	0.987 (0.002)	0
	N-SV		0.096 (0.000)	0.347 (0.001)	0.246 (0.001)	0.355 (0.000)	0.134 (0.001)	0.991 (0.001)	0
	LMSV		0.110	0.392	0.263	0.378	0.220	1.120	0
	SR-SV		0.089 (0.000)	0.341 (0.001)	0.236 (0.000)	0.336 (0.000)	0.131 (0.000)	0.951 (0.001)	6
RV	SV		0.087 (0.000)	1.370 (0.002)	0.206 (0.000)	0.319 (0.000)	0.118 (0.001)	0.625 (0.002)	0
	N-SV		0.087 (0.000)	1.368 (0.002)	0.206 (0.000)	0.317 (0.001)	0.117 (0.001)	0.627 (0.002)	1
	LMSV		0.100	1.418	0.224	0.342	0.195	0.742	0
	SR-SV		0.081 (0.000)	1.363 (0.002)	0.195 (0.000)	0.295 (0.000)	0.119 (0.001)	0.597 (0.001)	5

Table 18: TSX data: Forecast performance of the SR-SV and benchmark models using different realized measures. In each panel, the bold numbers indicate the best predictive scores.

References

- Andersen, T. G. and Bollerslev, T. (1998). Answering the skeptics: Yes, standard volatility models do provide accurate forecasts. *International Economic Review*, 39(4):885–905.
- Andersen, T. G., Dobrev, D., and Schaumburg, E. (2012). Jump-robust volatility estimation using nearest neighbor truncation. *Journal of Econometrics*, 169(1):75 – 93. Recent Advances in Panel Data, Nonlinear and Nonparametric Models: A Festschrift in Honor of Peter C.B. Phillips.
- Andrieu, C., Doucet, A., and Holenstein, R. (2010). Particle Markov chain Monte Carlo methods. *Journal of the Royal Statistical Society, Series B*, 72:1–33.
- Andrieu, C. and Roberts, G. (2009). The pseudo-marginal approach for efficient Monte Carlo computations. *The Annals of Statistics*, 37:697–725.
- Baillie, R. T., Bollerslev, T., and Mikkelsen, H. O. (1996). Fractionally integrated generalized autoregressive conditional heteroskedasticity. *Journal of Econometrics*, 74(1):3 – 30.
- Barndorff-Nielsen, O., Hansen, P., Lunde, A., and Shephard, N. (2008). Designing realized kernels to measure the ex post variation of equity prices in the presence of noise. *Econometrica*, 76(6):1481–1536. cited By 491.
- Barndorff-Nielsen, O. E. and Shephard, N. (2004). Power and Bipower Variation with Stochastic Volatility and Jumps. *Journal of Financial Econometrics*, 2(1):1–37.
- Bollerslev, T. (1986). Generalized autoregressive conditional heteroskedasticity. *Journal of Econometrics*, 31(3):307 – 327.
- Bollerslev, T. and Mikkelsen, H. O. (1996). Modeling and pricing long memory in stock market volatility. *Journal of Econometrics*, 73(1):151 – 184.
- Box, G. E. P. and Cox, D. R. (1964). An analysis of transformations. *Journal of the Royal Statistical Society: Series B (Methodological)*, 26(2):211–243.
- Breidt, F., Crato, N., and de Lima, P. (1998). The detection and estimation of long memory in stochastic volatility. *Journal of Econometrics*, 83(1):325 – 348.
- Cho, K., van Merriënboer, B., Gulcehre, C., Bahdanau, D., Bougares, F., Schwenk, H., and Bengio, Y. (2014). Learning phrase representations using RNN encoder–decoder for statistical machine translation. In *Proceedings of the 2014 Conference on Empirical Methods in Natural Language Processing (EMNLP)*, pages 1724–1734, Doha, Qatar. Association for Computational Linguistics.
- Crato, N. and de Lima, P. J. (1994). Long-range dependence in the conditional variance of stock returns. *Economics Letters*, 45(3):281 – 285.
- Del Moral, P. (2004). *Feynman-Kac Formulae: Genealogical and Interacting Particle Systems with Applications*. Springer, New York.

- Del Moral, P., Doucet, A., and Jasra, A. (2006). Sequential Monte Carlo samplers. *Journal of the Royal Statistical Society, Series B*, 68:411–436.
- Deligiannidis, G., Doucet, A., and Pitt, M. K. (2018). The correlated pseudo marginal method. *Journal of the Royal Statistical Society: Series B (Statistical Methodology)*, 80(5):839–870.
- Dieng, A. B., Ranganath, R., Altosaar, J., and Blei, D. M. (2018). Noisin: Unbiased regularization for recurrent neural networks.
- Ding, Z., Granger, C. W., and Engle, R. F. (1993). A long memory property of stock market returns and a new model. *Journal of Empirical Finance*, 1(1):83 – 106.
- Donaldson, R. G. and Kamstra, M. (1997). An artificial neural network-garch model for international stock return volatility. *Journal of Empirical Finance*, 4(1):17–46.
- Doornik, J. A. and Ooms, M. (2003). Computational aspects of maximum likelihood estimation of autoregressive fractionally integrated moving average models. *Computational Statistics and Data Analysis*, 42(3):333 – 348. Computational Econometrics.
- Duan, J.-C. and Fulop, A. (2015). Density-tempered marginalized Sequential Monte Carlo samplers. *Journal of Business & Economic Statistics*, 33(2):192–202.
- Elman, J. L. (1990). Finding structure in time. *Cognitive Science*, 14:179–21.
- Ferguson, T. S. (1973). A Bayesian analysis of some nonparametric problems. *The Annals of Statistics*, 1(2):209–230.
- Fleming, J., Kirby, C., and Ostdiek, B. (2003). The economic value of volatility timing using “realized” volatility. *Journal of Financial Economics*, 67(3):473 – 509.
- Garthwaite, P., Fan, Y., and Sisson, S. (2010). Adaptive optimal scaling of Metropolis-Hastings algorithms using the Robbins-Monro process. *Communications in Statistics - Theory and Methods*, 45.
- Gerber, M. and Chopin, N. (2014). Sequential Quasi-Monte Carlo. *Journal of the Royal Statistical Society: Series B (Statistical Methodology)*, 77.
- Giraitis, L., Kokoszka, P., Leipus, R., and Teyssi re, G. (2003). Rescaled variance and related tests for long memory in volatility and levels. *Journal of Econometrics*, 112(2):265 – 294.
- Goodfellow, I., Bengio, Y., and Courville, A. (2016). *Deep Learning*. MIT Press.
- Granger, C. W. J. and Joyeux, R. (1980). An introduction to long-memory time series models and fractional differencing. *Journal of Time Series Analysis*, 1(1):15–29.
- Gunawan, D., Dang, K., Quiroz, M., Kohn, R., and Tran, M. (2018). Subsampling sequential Monte Carlo for static Bayesian models. *arXiv:1805.03317*.
- Hansen, P. R. and Lunde, A. (2005). A forecast comparison of volatility models: does anything beat a GARCH(1,1)? *Journal of Applied Econometrics*, 20(7):873–889.

- Harvey, A. C. (2007). 16 - long memory in stochastic volatility. In Knight, J. and Satchell, S., editors, *Forecasting Volatility in the Financial Markets (Third Edition)*, Quantitative Finance, pages 351 – 363. Butterworth-Heinemann, Oxford.
- Higgins, M. L. and Bera, A. K. (1992). A class of nonlinear ARCH models. *International Economic Review*, 33(1):137–158.
- Hochreiter, S. and Schmidhuber, J. (1997). Long short-term memory. *Neural computation*, 9:1735–80.
- Hosking, J. R. M. (1981). Fractional differencing. *Biometrika*, 68(1):165–176.
- Jacquier, E., Polson, N. G., and Rossi, P. E. (1994). Bayesian analysis of stochastic volatility models (with discussion). *Journal of Business and Economic Statistics*, 12:371–417.
- Jeffreys, H. (1935). Some tests of significance, treated by the theory of probability. *Mathematical Proceedings of the Cambridge Philosophical Society*, 31(2):203–222.
- Jeffreys, H. (1961). *Theory of Probability*, 3rd. Clarendon Press, Oxford, England.
- Jensen, M. J. and Maheu, J. M. (2010). Bayesian semiparametric stochastic volatility modeling. *Journal of Econometrics*, 157(2):306 – 316.
- Kass, R. E., Carlin, B. P., Gelman, A., and Neal, R. M. (1998). Markov Chain Monte Carlo in practice: A roundtable discussion. *The American Statistician*, 52(2):93–100.
- Kass, R. E. and Raftery, A. E. (1995). Bayes factors. *Journal of the American Statistical Association*, 90(430):773–795.
- Kiliç, R. (2011). Long memory and nonlinearity in conditional variances: A smooth transition FIGARCH model. *Journal of Empirical Finance*, 18(2):368 – 378.
- Kim, H. Y. and Won, C. H. (2018). Forecasting the volatility of stock price index: A hybrid model integrating LSTM with multiple garch-type models. *Expert Systems with Applications*, 103:25 – 37.
- Kim, S., Shephard, N., and Chib, S. (1998). Stochastic volatility: likelihood inference and comparison with ARCH models. *Review of Economic Studies*, 65:361–393.
- Lipton, Z., Berkowitz, J., and Elkan, C. (2015). A critical review of recurrent neural networks for sequence learning. arXiv:1804.04359.
- Liu, J. S. and Chen, R. (1998). Sequential Monte Carlo methods for dynamic systems. *Journal of the American Statistical Association*, 93(443):1032–1044.
- Lo, A. W. (1991). Long-term memory in stock market prices. *Econometrica*, 59(5):1279–1313.
- Makridakis, S., Spiliotis, E., and Assimakopoulos, V. (2018). Statistical and machine learning forecasting methods: Concerns and ways forward. *PLOS ONE*, 13(3):1–26.
- Mandelbrot, B. (1967). The variation of some other speculative prices. *The Journal of Business*, 40(4):393–413.

- Martens, M. (2002). Measuring and forecasting S&P 500 index-futures volatility using high-frequency data. *Journal of Futures Markets*, 22(6):497–518.
- Neal, R. (2001). Annealed importance sampling. *Statistics and Computing*, 11:125–139.
- Nelson, D. B. (1991). Conditional heteroskedasticity in asset returns: A new approach. *Econometrica*, 59(2):347–370.
- Oliva, J. B., Póczos, B., and Schneider, J. G. (2017). The statistical recurrent unit. In *ICML2017*.
- Pagan, A. R. and Schwert, G. (1990). Alternative models for conditional stock volatility. *Journal of Econometrics*, 45(1):267 – 290.
- Pitt, M. K., dos Santos Silva, R., Giordani, P., and Kohn, R. (2012). On some properties of Markov chain Monte Carlo simulation methods based on the particle filter. *Journal of Econometrics*, 171(2):134 – 151. Bayesian Models, Methods and Applications.
- Poole, B., Sohl-Dickstein, J., and Ganguli, S. (2014). Analyzing noise in autoencoders and deep networks.
- Shephard, N. and Sheppard, K. (2010). Realising the future: forecasting with high-frequency-based volatility (heavy) models. *Journal of Applied Econometrics*, 25(2):197–231.
- Sietsma, J. and Dow, R. J. (1991). Creating artificial neural networks that generalize. *Neural Networks*, 4(1):67 – 79.
- Sowell, F. (1992). Maximum likelihood estimation of stationary univariate fractionally integrated time series models. *Journal of Econometrics*, 53(1):165 – 188.
- Taylor, S. (1986). *Modelling Financial Time Series*. John Wiley, Chichester.
- Taylor, S. J. (1982). Financial returns modelled by the product of two stochastic processes — a study of daily sugar prices 1961-79. In Anderson, O. D., editor, *Time Series Analysis: Theory and Practice*, page 203–226. Amsterdam: North-Holland.
- van Bellegem, S. (2012). Locally stationary volatility modeling. In Bauwens, L., Hafner, C., and Laurent, S., editors, *Volatility Models and Their Applications*. Wiley & Sons.
- Whittle, P. (1953). Estimation and information in stationary time series. *Ark. Mat.*, 2(5):423–434.
- Yu, J. (2002). Forecasting volatility in the New Zealand stock market. *Applied Financial Economics*, 12(3):193–202.
- Yu, J., Yang, Z., and Zhang, X. (2006). A class of nonlinear stochastic volatility models and its implications for pricing currency options. *Computational Statistics and Data Analysis*, 51(4):2218 – 2231.
- Zhang, G. (2003). Time series forecasting using a hybrid ARIMA and neural network model. *Neurocomputing*, 50:159 – 175.